[redacted]

Copy 74
RM H55A17

NACA RM H55A17

LIBRARY NACA - HSFS

RESEARCH MEMORANDUM

LATERAL STABILITY AND CONTROL CHARACTERISTICS OF THE CONVAIR XF-92A DELTA-WING AIRPLANE AS MEASURED IN FLIGHT

By Thomas R. Sisk and Duane O. Muhleman

High-Speed Flight Station
Edwards, Calif.

CLASSIFICATION CHANGED
TO Uncl.
BY AUTHORITY OF RA 124 Date 20 Jun 58
Ekerr 7-9-65

CLASSIFIED DOCUMENT

This material contains information affecting the National Defense of the United States within the meaning of the espionage laws, Title 18, U.S.C., Secs. 793 and 794, the transmission or revelation of which in any manner to an unauthorized person is prohibited by law.

NATIONAL ADVISORY COMMITTEE FOR AERONAUTICS

WASHINGTON

May 26, 1955

LIBRARY NACA - HSFS

[redacted]

LIBRARY NACA - MSFS

NATIONAL ADVISORY COMMITTEE FOR AERONAUTICS

RESEARCH MEMORANDUM

LATERAL STABILITY AND CONTROL CHARACTERISTICS OF THE CONVAIR XF-92A DELTA-WING AIRPLANE AS MEASURED IN FLIGHT

By Thomas R. Sisk and Duane O. Muhleman

SUMMARY

The lateral stability and control characteristics were investigated on the Convair XF-92A delta-wing airplane during the flights of the NACA research program. The investigation included sideslips, aileron rolls, and rudder pulses at altitudes ranging from 18,000 to 30,000 feet at indicated speeds from 160 to 420 miles per hour. A small amount of data is included with wing fences installed at 60 percent of the wing semispan for comparison with the basic airplane.

The lateral handling characteristics appear satisfactory when viewed in terms of gradually increasing sideslips, lateral control effectiveness, and period, and damping. The pilots objected to the over-all lateral handling characteristics, however, primarily because of the high roll-to-sideslip ratios which probably resulted from the relatively low static directional stability and relatively high effective dihedral. These adverse characteristics were aggravated at low speeds by high adverse yaw and rough air and at high speeds by high airplane response to small control deflections. The apparent high side force and poor hydraulic control system added to the objectional characteristics.

The lateral handling characteristics at low speeds were improved by the installation of wing fences. The improvement apparently resulted from an increase in the static directional stability.

INTRODUCTION

The Convair XF-92A airplane was originally constructed to determine the handling characteristics, primarily at low speed, of an airplane having a delta-wing configuration. In view of the interest in delta-wing airplanes for high-speed flight, a larger power plant was installed

LIBRARY NACA - MSFS

in the XF-92A and the flight envelope was extended to sonic speed during joint testing by the National Advisory Committee for Aeronautics and the Air Force. The results of this investigation are presented in references 1 to 3. Upon completion of these tests the XF-92A was assigned to the NACA High-Speed Flight Station for general research.

All the pilots who have flown the XF-92A (during the joint NACA—Air Force program and the NACA research program) have reported that the airplane exhibited poor lateral handling characteristics, particularly at low speed. The present paper presents the lateral stability and control characteristics of the XF-92A as determined from sideslips, aileron rolls, and rudder pulses. Wing fences were installed on the XF-92A at 60 percent of the wing semispan to evaluate the longitudinal maneuvering stability characteristics with this modification (ref. 4), and a limited amount of lateral data is presented herein with the fence configuration for comparison with the basic airplane. The tests were performed at the NACA High-Speed Flight Station at Edwards, Calif.

SYMBOLS

A_Y transverse acceleration factor, g units

b wing span, ft

c wing chord, ft

C_l rolling-moment coefficient, $\frac{\text{Rolling moment}}{qSb}$

C_n yawing-moment coefficient, $\frac{\text{Yawing moment}}{qSb}$

C_{N_A} airplane normal-force coefficient, Wn/qS

C_Y lateral-force coefficient, $A_Y W/qS$

$C_{1/2}$ cycles-to-damp to one-half amplitude

g acceleration due to gravity, ft/sec^2

h_p pressure altitude, ft

I_X moment of inertia about longitudinal stability axis, slug-ft^2

I_{XZ}	product of inertia, slug-ft^2
I_Z	moment of inertia about normal stability axis, slug-ft^2
M	Mach number
n	normal acceleration factor, g units
P	period, sec
p	rolling angular velocity, radians/sec
pb/2V	wing-tip helix angle, radians
$\frac{pb}{2V}/\delta_a$	variation of wing-tip helix angle with lateral control angle, per deg
q	dynamic pressure, lb/ft^2
q	pitching angular velocity, radians/sec
r	yawing angular velocity, radians/sec
S	wing area, sq ft
$T_{1/2}$	time-to-damp to one-half amplitude, sec
t	time, sec
V	true velocity, ft/sec
V_e	equivalent side velocity, $(v\sqrt{\sigma})$, ft/sec
V_i	indicated velocity, mph
v	side velocity, $\frac{\beta V}{57.3}$, ft/sec
α	angle of attack, deg
β	sideslip angle, deg
δ_a	lateral control angle, $\delta_{e_L} - \delta_{e_R}$, deg

δ_e longitudinal control angle, $\frac{\delta_{e_L} + \delta_{e_R}}{2}$, deg

δ_r rudder control angle, deg

ϵ angle of principal axis of inertia from body axis, positive when principal axis is below body axis, deg

Λ angle of sweepback, deg

σ air-density ratio

ϕ bank angle, deg

C_{l_β} variation of rolling-moment coefficient with angle of sideslip, $dC_l/d\beta$, per radian

C_{l_p} damping in roll, $dC_l/d\,\frac{pb}{2V}$, per radian

C_{n_β} variation of yawing-moment coefficient with angle of sideslip, $dC_n/d\beta$, per radian

C_{Y_β} variation of lateral-force coefficient with angle of sideslip, $dC_Y/d\beta$, per radian

$dA_Y/d\beta$ variation of transverse acceleration factor with angle of sideslip, g/deg

$d\delta_a/d\beta$ variation of lateral control angle with angle of sideslip

$d\delta_r/d\beta$ variation of rudder control angle with angle of sideslip

Subscripts:

L left

R right

max maximum

AIRPLANE

The Convair XF-92A is a semitailless delta-wing airplane having 60° leading-edge sweepback of the wing and vertical stabilizer. The elevons and rudder are full-span constant-chord surfaces and are 100 percent hydraulically boosted. The artificial feel system provided has forces approximately proportional to deflection and are adjustable in flight by the pilot. The airplane has no leading- or trailing-edge slats or flaps, no dive brakes, and no trim tabs. Wing fences were installed at 60 percent of the wing semispan for part of the tests presented in this paper.

Table I lists the physical characteristics and figure 1 shows photographs of the airplane. A three-view drawing of the airplane is presented in figure 2. Figure 3 presents a sketch of the wing-fence configuration that was installed during part of the tests presented in this paper.

INSTRUMENTATION AND ACCURACY

The XF-92A airplane is equipped with standard NACA recording instruments for recording the quantities pertinent to this investigation. All instruments are correlated by a common timer.

The airspeed installation was calibrated by using the radar photo-theodolite method of reference 5. The low-speed static pressure calibration needed for the pressure survey in the method was obtained from an Air Force F-86 pacer airplane and the pressure surveys were checked with data obtained from radiosonde balloons released at the time of the flights. This calibration method resulted in a Mach number error of about 1 percent.

Accuracies of the pertinent quantities are:

p, radians per sec	± 0.10
r, radians per sec	± 0.02
ϕ, deg	± 10.0
β, deg	± 0.50
δ_a, deg	± 0.20
δ_r, deg	± 0.20
V_i, mph	± 4.0

TESTS, RESULTS, AND DISCUSSION

The lateral stability and control characteristics were measured in gradually increasing sideslips, rudder-fixed aileron rolls, and rudder pulses over the altitude range from 18,000 to 30,000 feet at indicated speeds from about 160 to 420 mph ($M \approx 0.30$ to 0.94). All the pilots who have flown the XF-92A have objected to the lateral handling characteristics, particularly at the lower speeds, and therefore the majority of the data were obtained below an indicated speed of 250 mph ($M < 0.50$). The higher speed range was not covered as fully as might be desired because the research program was terminated abruptly when the airplane sustained considerable damage as a result of a nosewheel strut failure while taxiing. The data are presented for various indicated speeds in this paper since the lower speed range is the region of primary interest. A limited amount of lateral data was obtained with wing fences installed at 60 percent of the wing semispan and is presented for comparison with the basic airplane. The center of gravity for these tests varied between 27.2 and 28.7 percent of the mean aerodynamic chord.

Static Lateral Stability

The static lateral stability data obtained from gradually increasing sideslips are presented in figures 4 to 7. Figure 4 presents representative variations of control positions and transverse acceleration with angle of sideslip for the basic airplane, clean and gear down, over the speed range tested. Figure 4 shows that the pitching moment resulting from sideslip is small and the variation of rudder control angle and lateral control angle with sideslip is linear over the entire range of sideslip angles covered. These data are summarized in figure 5 which shows that, for the clean configuration, the variation of lateral-force coefficient with angle of sideslip C_{Y_β}, as obtained from the expression $C_{Y_\beta} = W \frac{dA_Y}{d\beta/qS}$ has little variation with speed as the indicated speed increases from about 150 to 440 mph. The rudder required to sideslip $d\delta_r/d\beta$ increases from a value of 0.40 to 0.55, and the aileron required to maintain constant heading $d\delta_a/d\beta$ decreases from a value of 0.90 to 0.30. Lowering the gear increases the lateral-force coefficient, decreases the apparent directional stability as indicated by $d\delta_r/d\beta$, and increases the dihedral effect $d\delta_a/d\beta$, the magnitude of increase or decrease being generally small and relatively constant with speed for each parameter. Figures 6 and 7 present data similar to

figures 4 and 5 with wing fences installed. Only low-speed data were obtained with the fence configuration and it appears that in this speed range the only appreciable difference between the two configurations is that with the fences installed the apparent directional stability is increased at the lowest speeds, more rudder being required to sideslip. There is a rapid increase of apparent dihedral effect as the speed decreases for both the basic airplane and the fence configurations.

Lateral Control

The lateral control data obtained from rudder-fixed aileron rolls are presented in figures 8 to 13. Figure 8 presents the variation of wing-tip helix angle with lateral control angle for the basic airplane, clean and gear down, and shows that this variation is linear with control deflection over the range of deflections tested. These data are summarized in figure 9 which shows that $\frac{pb}{2V}/\delta_a$ for the clean airplane varies from a value of 0.0050 at V_i = 170 mph to 0.0095 at V_i = 420 mph, the largest change being noted at the lower speeds. Lowering the gear reduces the value of $\frac{pb}{2V}/\delta_a$. Figures 10 and 11 present data similar to figures 8 and 9 with wing fences installed. Again, the fence data are meager, but figure 11 indicates that installing the fences does not appreciably change the value of $\frac{pb}{2V}/\delta_a$. The pilot reported adequate aileron control for both configurations over the entire speed range tested.

Figure 12 presents representative time histories of six aileron rolls to illustrate the reduction in $\frac{pb}{2V}/\delta_a$ at the lower speeds. Figures 12(a) and 12(b) illustrate the high-speed case where the trim angle of attack is of the order of 3°. These rolls show the more or less conventional slow development of adverse yaw during the roll. Figures 12(c) and 12(d) illustrate the low-speed case for the airplane, clean and gear down, respectively, for trim angles of attack of approximately 12°. At these high angles of attack, the sideslip angle increases immediately with roll apparently as a result of rolling about the principal axis. This sideslip then reduces the peak rolling velocity. The rapid development of sideslip is very bothersome to the pilot. Figures 12(e) and 12(f) illustrate that the fence configuration at low speed, clean and gear down, differs little from the basic airplane configuration.

The bank-angle data obtained from the aileron rolls are presented in figure 13. Figure 13(a) shows the variation of maximum rolling velocity, time to reach a bank angle of 90° and the bank angle at

maximum rolling velocity for one-third, one-half, and two-thirds aileron deflection. Reference 6 recommends a tentative high-speed criterion based on a time of 1.0 second to reach a bank angle of 90°. It may be seen that the XF-92A meets this criterion at indicated speeds above about 260 mph with two-thirds aileron deflection. Figure 13(b) compares the basic airplane, gear down, with the clean configuration and figures 13(c) and 13(d) compare the fence configuration, clean and gear down, with the basic airplane. Lowering the gear on the basic airplane reduces the maximum rolling velocity and, at the lower speeds, increases the time to reach a bank angle of 90°. No appreciable differences can be noted between the basic airplane clean and the fence configuration clean. Lowering the gear on the fence configuration decreases the time to reach a bank angle of 90° at the lower speeds as compared with the basic airplane, gear down.

Dynamic Lateral Stability

Rudder pulses were performed at altitudes of approximately 20,000 and 30,000 feet, clean and gear down, with the basic airplane and with the fence configuration, and the results of these data are presented in figures 14 and 15. No difference could be distinguished between the gear configuration or the two altitudes for the speed range where there are overlapping data; therefore, figure 14(a) presents the variation of period and time to damp to one-half amplitude with indicated speed for the basic airplane. These data were evaluated during the portion of the maneuver in which all controls were held fixed. Figure 14(a) shows that the period decreases from a value of approximately 4.0 seconds to 2.5 seconds as the speed increases from 160 to 360 mph. The time to damp to one-half amplitude is essentially constant over this speed range with a value of approximately 1.75 seconds. Figure 14(b) presents the fence-configuration data for comparison with the basic airplane. This figure shows that the only effect of the fences is to decrease the time to damp slightly in the restricted speed range for which a comparison is possible.

The primary objection to the handling characteristics appears to lie in the large roll-to-sideslip ratios experienced during directional maneuvers. Reference 7 proposed a tentative criterion based on the reciprocal of the cycles-to-damp to one-half amplitude and the roll-to-sideslip ratio. The handling-qualities requirements of reference 8 specify satisfactory dynamic lateral stability based on such a criterion. This specification is presented in figure 15, together with data from tests made with the XF-92A airplane both with and without wing fences. From this figure it may be seen that the dynamic lateral stability of

the XF-92A airplane is generally in the unsatisfactory region. The points for the basic configuration generally lie deeper in the unsatisfactory range than do the points for the fence configuration. This indicated improvement in lateral behavior attributable to fences was borne out by pilots' comments. According to pilots' comments, this high roll-to-sideslip ratio is aggravated by rough air at the lower speeds and by the high airplane response to small control deflections at the higher speeds. Figure 16 illustrates the unsteadiness resulting from this response during an attempted trim run over the Mach number range from 0.82 to 0.89.

Calculation of C_{l_β}, C_{n_β}, and C_{Y_β}

The variations of the effective dihedral parameter C_{l_β}, the directional stability parameter C_{n_β}, and the lateral-force parameter C_{Y_β}, with indicated speed for the basic airplane, clean, at an altitude of 20,000 feet were determined from the following equations:

$$C_{l_\beta} = \left(\frac{d\frac{pb}{2V}}{d\delta_a}\right)\left(\frac{d\delta_a}{d\beta}\right) C_{l_p}$$

$$C_{n_\beta} = \frac{I_Z}{qSb}\left[\left(\frac{2\pi}{P}\right)^2 + \left(\frac{0.693}{T_{1/2}}\right)^2\right] - C_{l_\beta}\left(\frac{I_{XZ}}{I_X}\right)$$

$$C_{Y_\beta} = \frac{W\left(\frac{dA_Y}{d\beta}\right)}{qS}$$

In determining C_{l_β}, the coefficients of $d\frac{pb}{2V}/d\delta_a$ and $d\delta_a/d\beta$ were obtained from the flight-test data of the aileron rolls and sideslips, respectively, and the value of C_{l_p} of -0.2 was obtained from reference 9. In determining C_{n_β}, the values for P and $T_{1/2}$ were obtained from flight rudder pulses and the inertia terms I_Z and I_X and the principal axis inclination ($\epsilon = 1^\circ$) were obtained from the contractor.

(The inertia values used in the calculations are tabulated in table II.) In determining C_{Y_β}, the controls-fixed portion of the rudder pulses were used to determine the variation of the transverse acceleration factor with sideslip angle. It is understood that the equations listed above will not yield true static derivatives, particularly in the case of C_{l_β}, since dynamic flight data were used in the equations. It is felt, however, that the equations yield adequate approximations to illustrate the comparisons discussed in this section.

The results of these calculations are presented in figure 17. This figure shows that C_{l_β} varies between values of -0.05 to -0.04 per radian in the speed range from 160 to 380 mph. Over this same speed range, C_{n_β} decreases from a value of 0.06 to 0.04 per radian and C_{Y_β} decreases from a value of -0.75 to -0.65 per radian. It may be noted that the values of C_{Y_β} obtained from sideslips (fig. 5) are considerably lower than the values obtained from the controls-fixed portion of the rudder pulses. The major difference between the two values probably results from the contribution of the aileron and rudder deflections required for the sideslip maneuvers. Also shown in figure 17 for comparison are the values of C_{l_β}, C_{n_β}, and C_{Y_β} from Ames full-scale wind-tunnel tests (unpublished) for the basic airplane adjusted to the lift coefficients and trim elevon angles corresponding to indicated speeds of 145, 180, and 220 mph. These data show excellent agreement in C_{n_β} and C_{Y_β}. The flight-determined values of C_{l_β} are considerably lower than the wind-tunnel data at the lower speeds because of the effects of adverse yaw in causing a reduction in $\frac{pb}{2V}/\delta_a$ used in the calculations. The calculations for the fence configuration presented in figure 17 show the static directional stability to be increased approximately 40 percent over the value for the basic airplane at the lowest speed.

This increase in directional stability attributable to the fences is considerably greater than the effect on the apparent stability parameter $d\delta_r/d\beta$, (fig.7). It should be noted that the value of C_{n_β} determined from the pulse data is primarily sensitive to the period. Inasmuch as there is considerable scatter shown in the period for the rather limited fence data the absolute value of the directional stability parameter may be questionable.

LIBRARY NACA - HSFS

Although the parameters of figure 17 appear normal, a further analysis indicates that they are not in the proper order of magnitude with respect to each other for best stability. This is illustrated in figure 18. Figure 18(a) presents the variation of the ratio of C_{n_β} to C_{l_β} with lift coefficient and indicated speed as determined from the curves of figure 17. Also shown on figure 18(a) for comparison with the XF-92A are representative points for the X-5 (refs. 10, 11, and unpublished data), a 35° swept-wing airplane (ref. 12), and the D-558-II (unpublished data). It may be seen that the ratio of C_{n_β} to C_{l_β} $\left(C_{n_\beta}/C_{l_\beta} \approx 1\right)$ for the XF-92A is generally less than the ratio for other airplanes. It follows that, for satisfactory handling characteristics, the XF-92A would require a higher ratio of C_{n_β} to C_{l_β} than required for airplanes of higher aspect ratio (as predicted in ref. 13). Note that the X-5 airplane ($\Lambda = 59^\circ$, aspect ratio = 2.2) has a considerably higher ratio of C_{n_β} to C_{l_β} than the XF-92A except at the lower speeds. Figure 18(b) presents the same comparison for the ratio of C_{Y_β} to C_{n_β}. It may be seen from figure 18(b) that the ratio for the XF-92A is of the order of three to four times the magnitude of the ratio for the other airplanes. This high apparent lateral force probably contributes to the pilots' impressions of the poor handling qualities.

The NACA pilot reported an improvement in the handling qualities with the installation of wing fences. The only appreciable difference that can be noted in the static parameters with the fences installed is the increased static directional stability shown in figures 17 and 7. Although the magnitude of the increase in C_{n_β} may be somewhat questionable because of the scatter in the data the change is in the direction to improve the ratios as shown in figure 18.

Control System

Finally, part of the difficulties encountered on the XF-92A may be attributed to the poor hydraulic control system. Evaluation of ground calibrations has shown the control system to have high friction and breakout forces and appreciable lag of surface-to-stick motion. These characteristics are particularly objectionable at low speeds where large control deflections are required to maneuver and also at high speeds where the airplane is sensitive to small control displacements.

LIBRARY NACA - HSFS

CONCLUSIONS

The results obtained from sideslips, aileron rolls, and rudder pulses performed at altitudes ranging from 18,000 to 30,000 feet at indicated speeds from 160 to 420 mph during the flights of the NACA research program of the XF-92A airplane indicate the following conclusions:

1. The static lateral stability characteristics as measured in sideslips appear satisfactory although there is a rapid increase in apparent dihedral effect at the lower speeds. There is adequate rudder power over the entire speed range tested.

2. The lateral control as measured in aileron rolls appears adequate over the entire speed range tested although there is a considerable reduction in aileron effectiveness at the lower speeds.

3. The dynamic lateral stability of the airplane was generally in the unsatisfactory region when compared to U. S. Air Force requirements for satisfactory values of reciprocal of cycles to damp to half amplitude and ratio of roll angle to sideslip velocity.

4. Although the airplane appeared to have satisfactory static lateral stability and control characteristics, the pilots objected to the over-all lateral handling characteristics primarily because of the high roll-to-sideslip ratios which probably resulted from the relatively low static directional stability and relatively high effective dihedral. These adverse characteristics were aggravated at low speeds by high adverse yaw and rough air and at high speeds by high airplane response to small control deflections. The apparent high side force and poor hydraulic control system added to the objectional characteristics.

5. Installing wing fences on the airplane improved the handling characteristics at the lower speeds, in the pilots' opinion, probably because of the increase in static directional stability attributable to the fences.

High-Speed Flight Station,
National Advisory Committee for Aeronautics,
Edwards, Calif., January 10, 1955.

REFERENCES

1. Sisk, Thomas R., and Mooney, John M.: Preliminary Measurements of Static Longitudinal Stability and Trim for the XF-92A Delta-Wing Research Airplane in Subsonic and Transonic Flight. NACA RM L53B06, 1953.

2. Holleman, Euclid C., Evans, John H., and Triplett, William C.: Preliminary Flight Measurements of the Dynamic Longitudinal Stability Characteristics of the Convair XF-92A Delta-Wing Airplane. NACA RM L53E14, 1953.

3. Bellman, Donald R., and Sisk, Thomas R.: Preliminary Drag Measurements of the Consolidated Vultee XF-92A Delta-Wing Airplane in Flight Tests to a Mach Number of 1.01. NACA RM L53J23, 1954.

4. Sisk, Thomas R., and Muhleman, Duane O.: Longitudinal Stability Characteristics in Maneuvering Flight of the Convair XF-92A Delta-Wing Airplane Including the Effects of Wing Fences. NACA RM H54J27, 1954.

5. Zalovcik, John A.: A Radar Method of Calibrating Airspeed Installations on Airplanes in Maneuvers at High Altitudes and at Transonic and Supersonic Speeds. NACA Rep. 985, 1950. (Supersedes NACA TN 1979.)

6. Williams, W. C., and Crossfield, A. S.: Handling Qualities of High Speed Airplanes. NACA RM L52A08, 1952.

7. Liddell, Charles J., Jr., Creer, Brent Y., and Van Dyke, Rudolph D., Jr.: A Flight Study of Requirements for Satisfactory Lateral Oscillatory Characteristics of Fighter Aircraft. NACA RM A51E16, 1951.

8. Anon.: Military Specifications - Flying Qualities of Piloted Airplanes. MIL-F-8785 (ASG), Sept. 1, 1954. (Amendment - 1, Oct. 19, 1954.)

9. Jaquet, Byron M., and Brewer, Jack D.: Effects of Various Outboard and Central Fins on Low-Speed Static-Stability and Rolling Characteristics of a Triangular-Wing Model. NACA RM L9E18, 1949.

10. Kemp, William B., Jr., and Becht, Robert E.: Stability and Control Characteristics at Low Speed of a 1/4-Scale Bell X-5 Airplane Model - Lateral and Directional Stability and Control. NACA RM L50C17a, 1950.

11. Childs, Joan M.: Flight Measurements of the Stability Characteristics of the Bell X-5 Research Airplane in Sideslips at 59° Sweepback. NACA RM L52K13b, 1953.

12. Triplett, William C., and Brown, Stuart C.: Lateral and Directional Dynamic Response Characteristics of a 35° Swept-Wing Airplane as Determined from Flight Measurements. NACA RM A52I17, 1952.

13. McKinney, Marion O., Jr., and Shanks, Robert E.: Lateral Stability and Control Characteristics of a Free-Flying Model Having an Unswept Wing With an Aspect Ratio of 2. NACA TN 1658, 1948.

TABLE I

PHYSICAL CHARACTERISTICS OF THE XF-92A AIRPLANE

Wing:	
Area, sq ft	425
Span, ft	31.33
Airfoil section	NACA $65_{(06)}$-006.5
Wing-panel area, outboard of root strain-gage station, sq ft	137.1
Mean aerodynamic chord, ft	18.09
Aspect ratio	2.31
Root chord, ft	27.13
Tip chord	0
Taper ratio	0
Sweepback (leading edge), deg	60
Incidence, deg	0
Dihedral (chord plane), deg	0
Elevons:	
Area (total, both, aft of hinge line), sq ft	76.19
Span (one elevon), ft	13.35
Chord (aft of hinge line, constant except at tip), ft	3.05
Movement, deg	
Elevator:	
Up	15
Down	5
Aileron, total	10
Operation	Hydraulic
Vertical tail:	
Area, sq ft	75.35
Height, above fuselage center line, ft	11.50
Rudder:	
Area, sq ft	15.53
Span, ft	9.22
Travel, deg	±8.5
Operation	Hydraulic
Fuselage:	
Length, ft	42.80
Power plant:	
Engine	Allison J33-A-29 with afterburner
Rating:	
Static thrust at sea level, lb	5,600
Static thrust at sea level with afterburner, lb	7,500
Weight:	
Gross weight (560 gal fuel), lb	15,560
Empty weight, lb	11,808
Center-of-gravity locations:	
Gross weight (560 gal fuel), percent M.A.C.	25.5
Empty weight, percent M.A.C.	29.2
Moment of inertia in pitch, slug-ft^2	35,000

TABLE II

INERTIA VALUE FOR XF-92A AIRPLANE

$[\epsilon = 1^{\circ}]$

α, deg	I_Z, slug-ft^2	I_{XZ}/I_X
0	------	-----
2	38,600	-0.10
4	38,500	-.30
6	38,350	-.48
8	38,050	-.63
10	37,750	-.76
12	37,350	-.87
14	36,850	-.95
16	36,300	-1.01
18	35,700	-1.05
20	35,050	-1.08

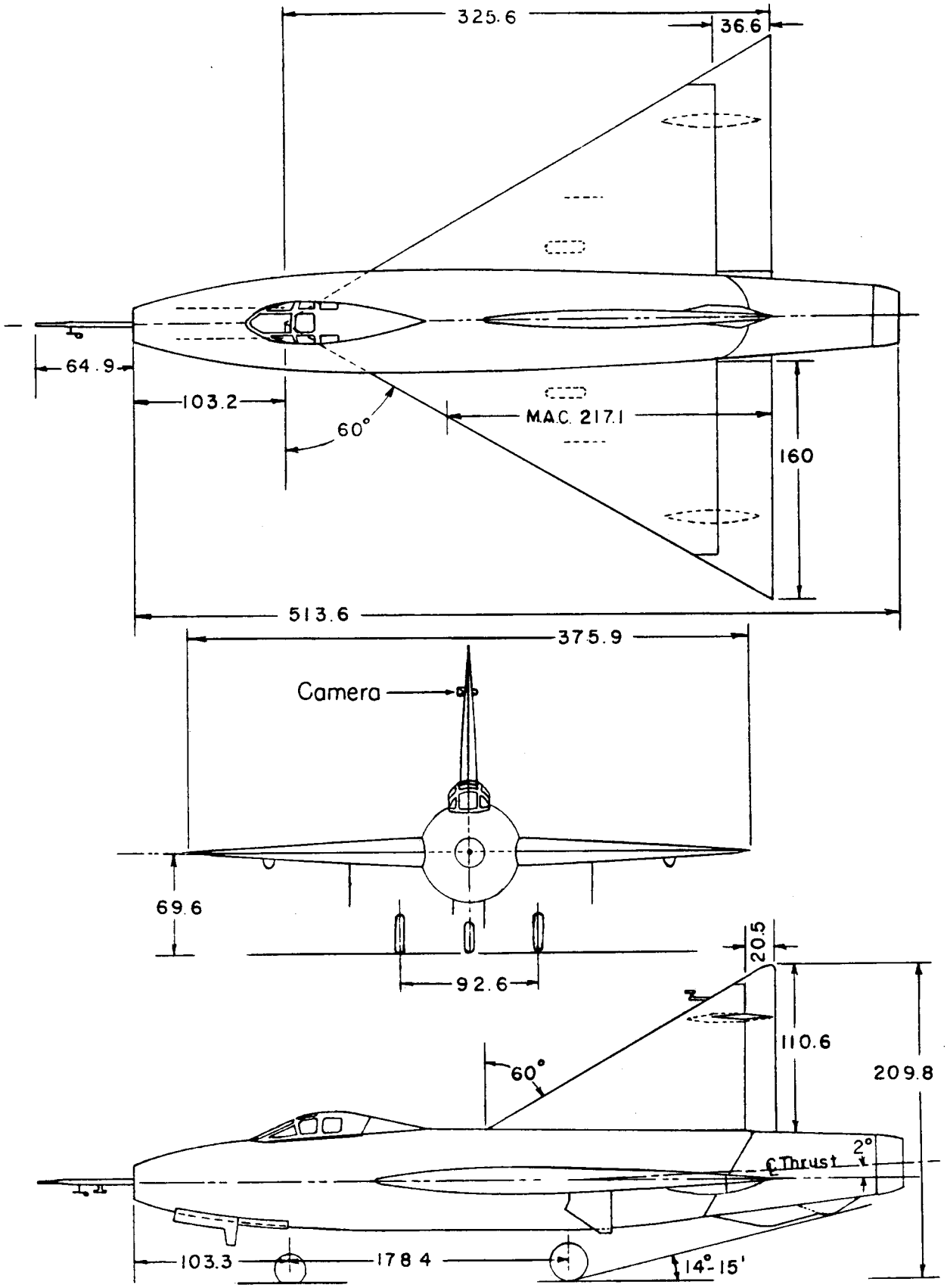

Figure 1.- Three-view drawing of the XF-92A airplane. All dimensions in inches.

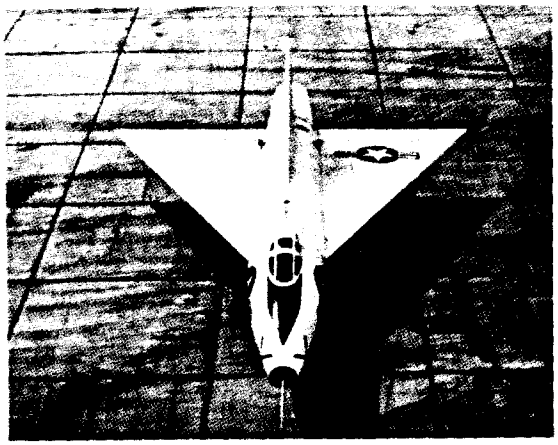

(a) Overhead front view.

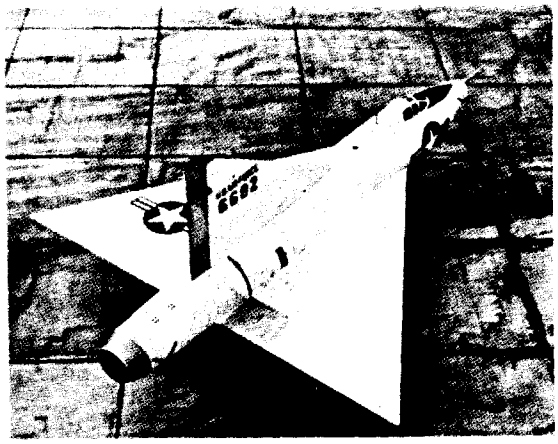

(b) Three-quarter rear view.

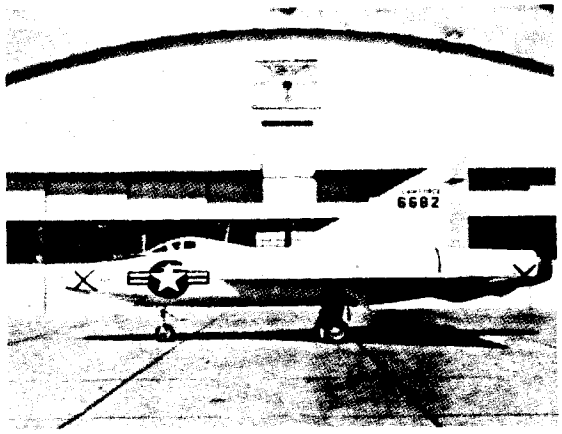

(c) Left side view.

L-81260

Figure 2.- Photographs of XF-92A research airplane.

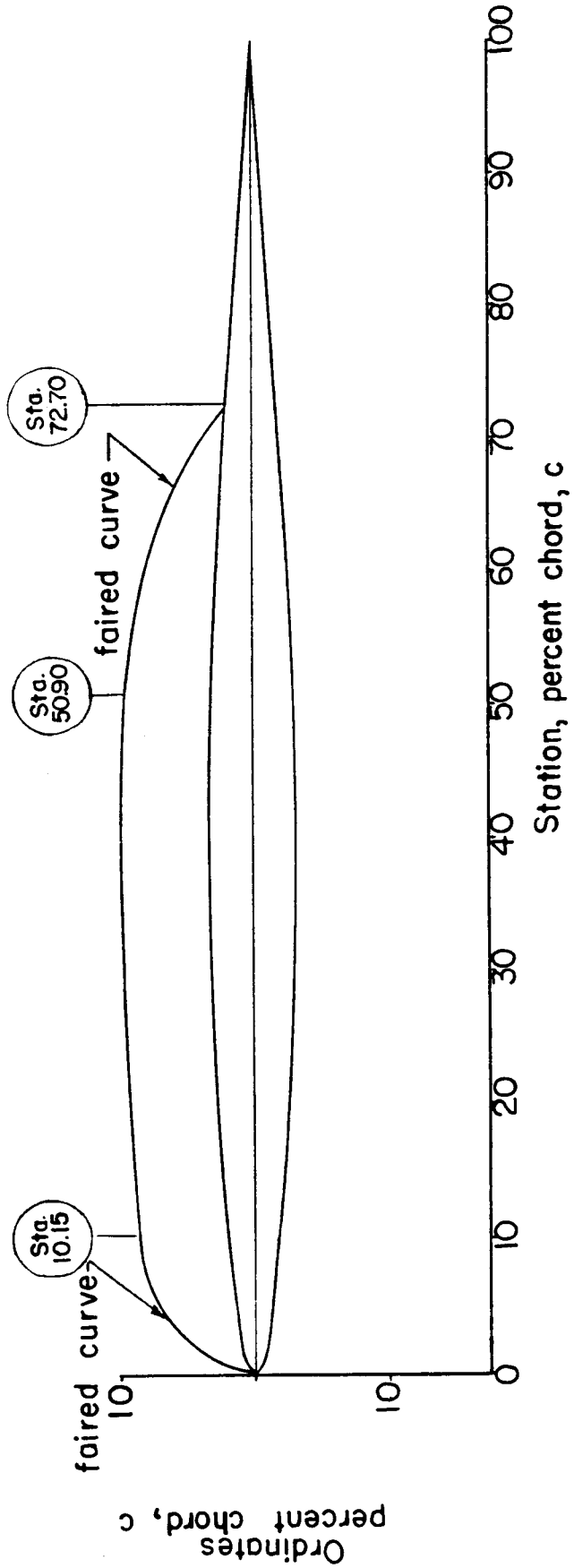

Figure 3.- Wing fence configuration.

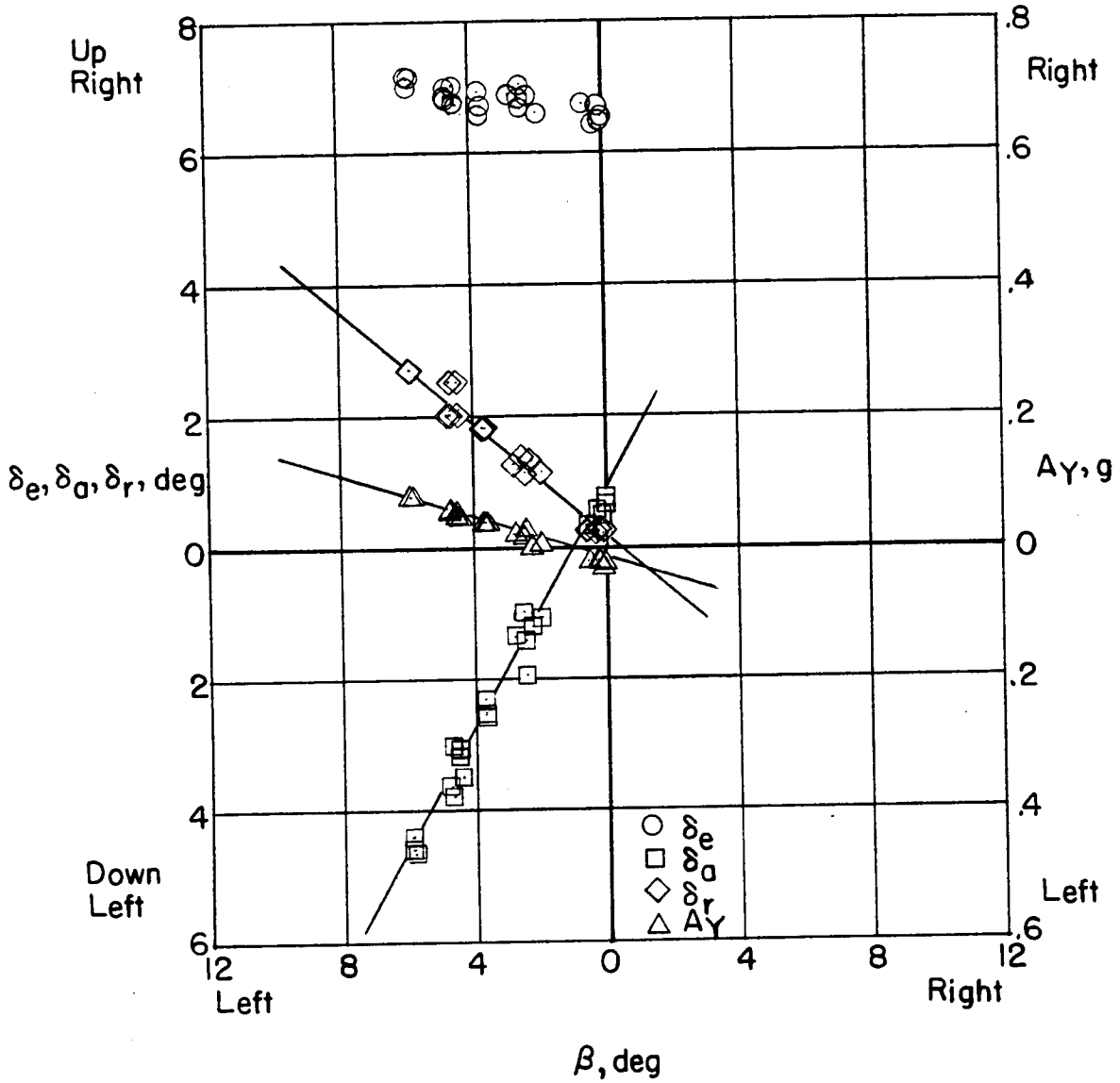

(a) V_i = 145 mph; α = 17.2°; C_{N_A} = 0.60; clean.

Figure 4.- Variation of control positions and transverse acceleration factor with angle of sideslip for the basic airplane.

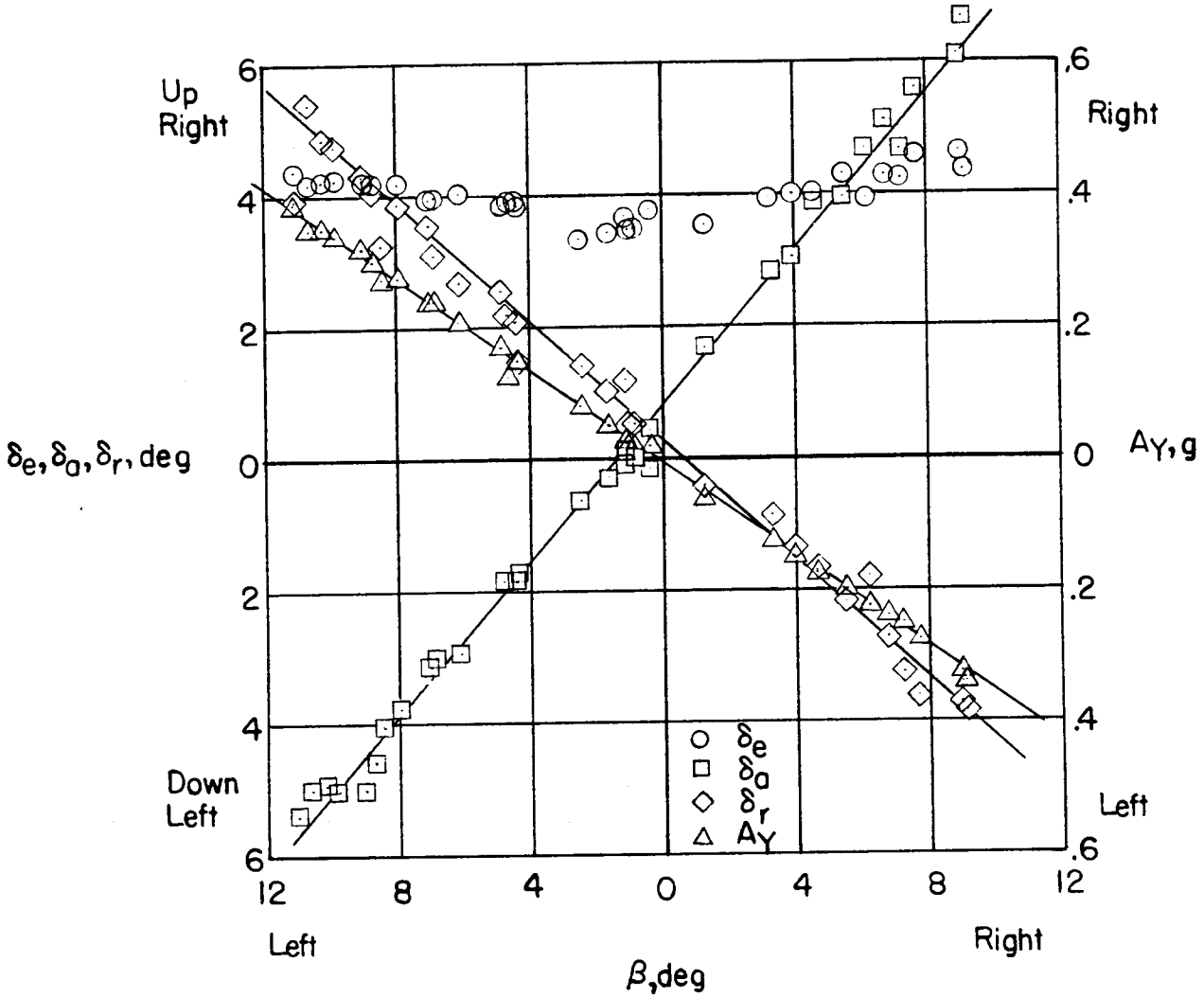

(b) V_i = 205 mph; α = 7.9°; C_{N_A} = 0.20; clean.

Figure 4.- Continued.

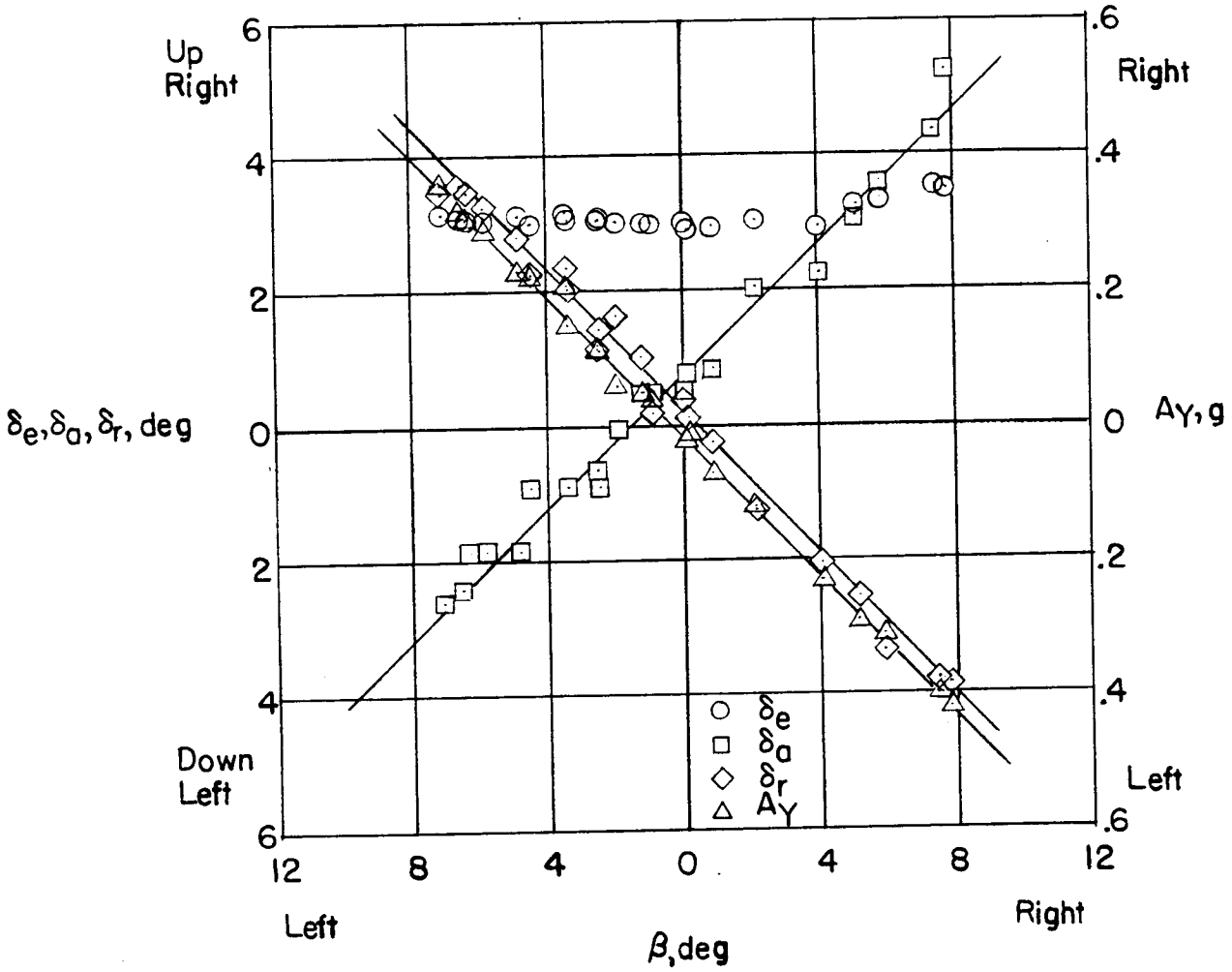

(c) V_i = 205 mph; $\alpha = 5.6^{\circ}$; C_{N_A} = 0.20; clean.

Figure 4.- Continued.

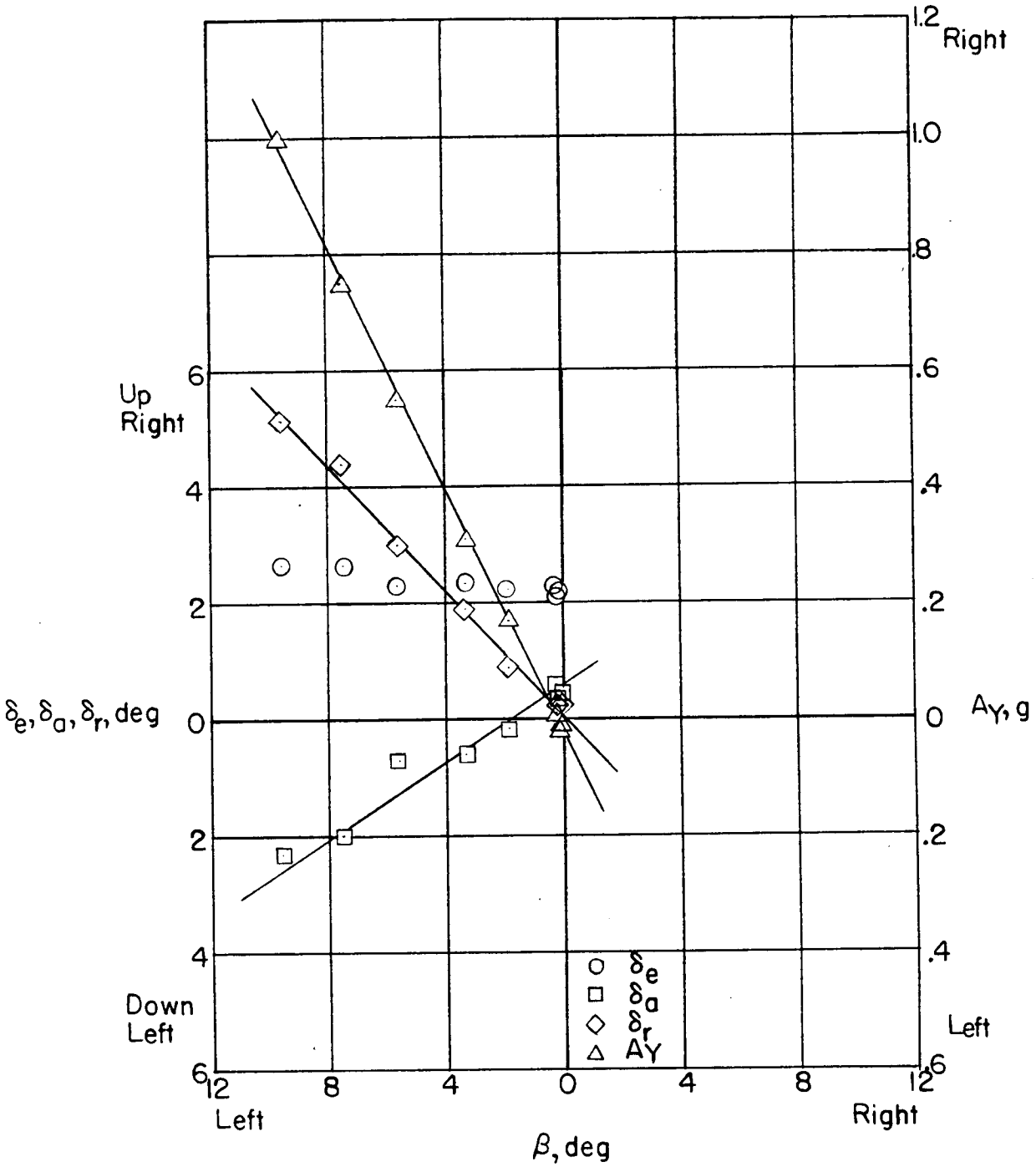

(d) V_i = 378 mph; α = 2.3°; C_{N_A} = 0.09; clean.

Figure 4.- Continued.

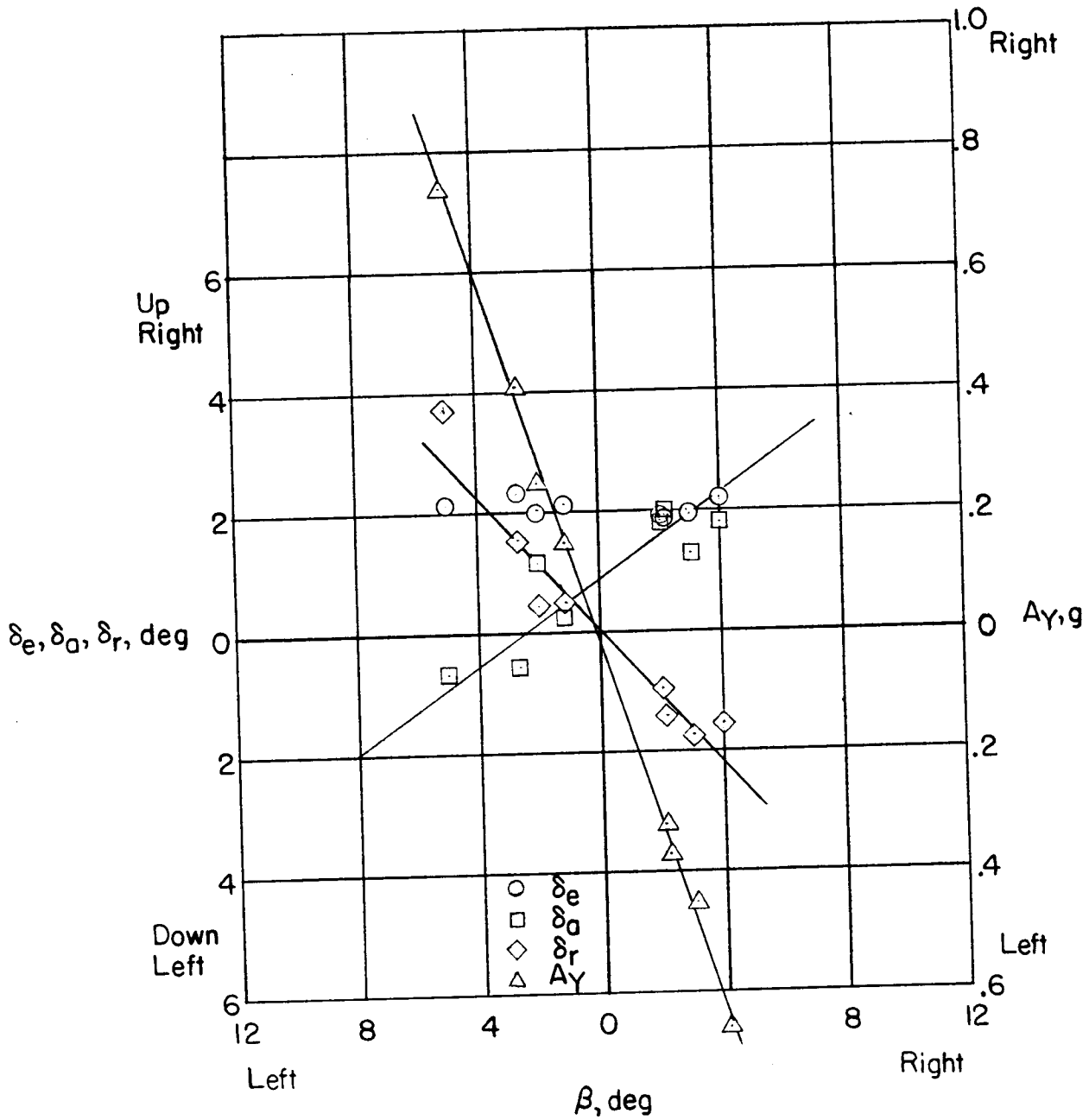

(e) V_i = 438 mph; α = 2.0°; C_{N_A} = 0.08; clean.

Figure 4.- Continued.

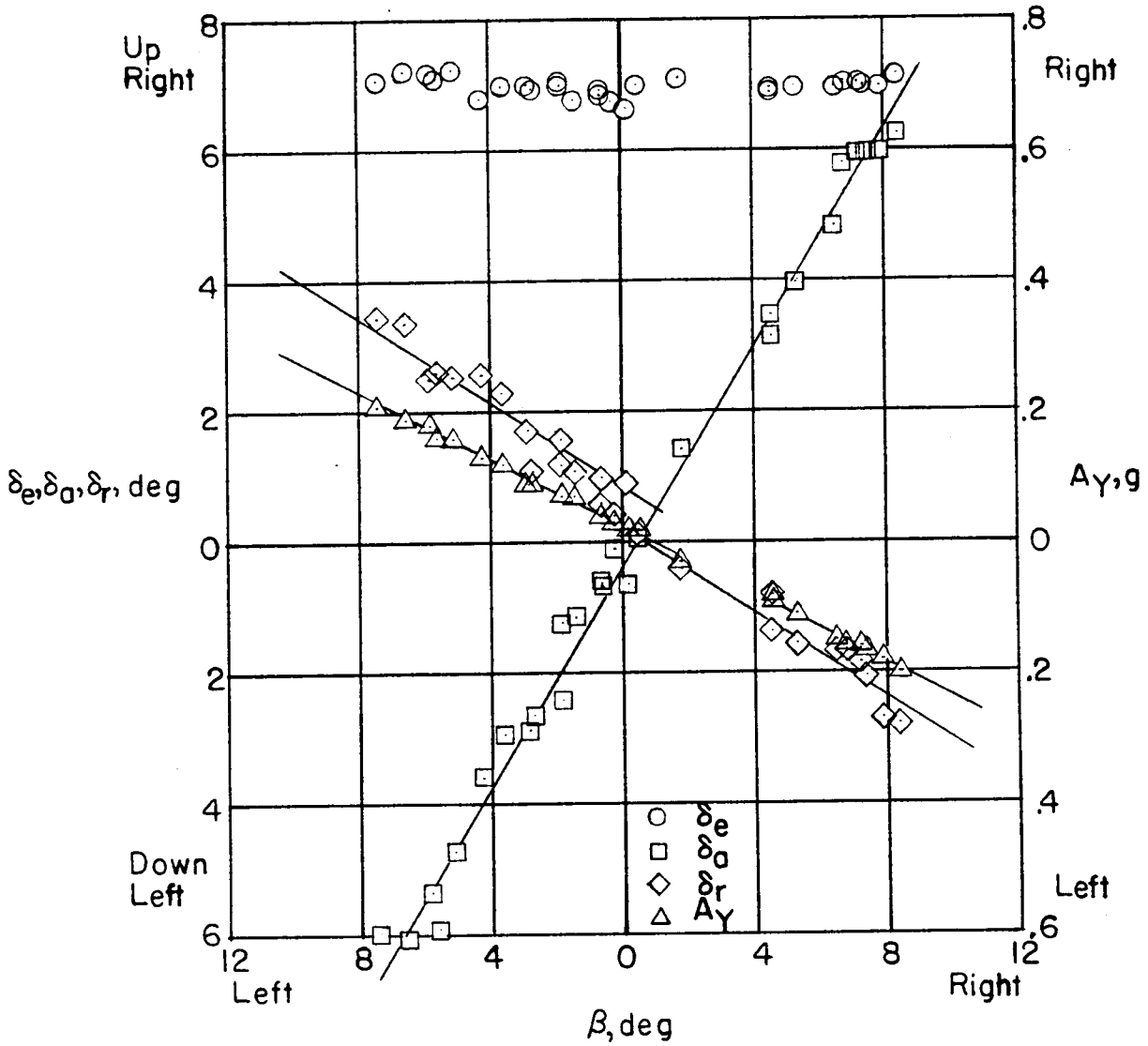

(f) V_i = 163 mph; α = 14.6°; C_{N_A} = 0.49; gear down.

Figure 4.- Continued.

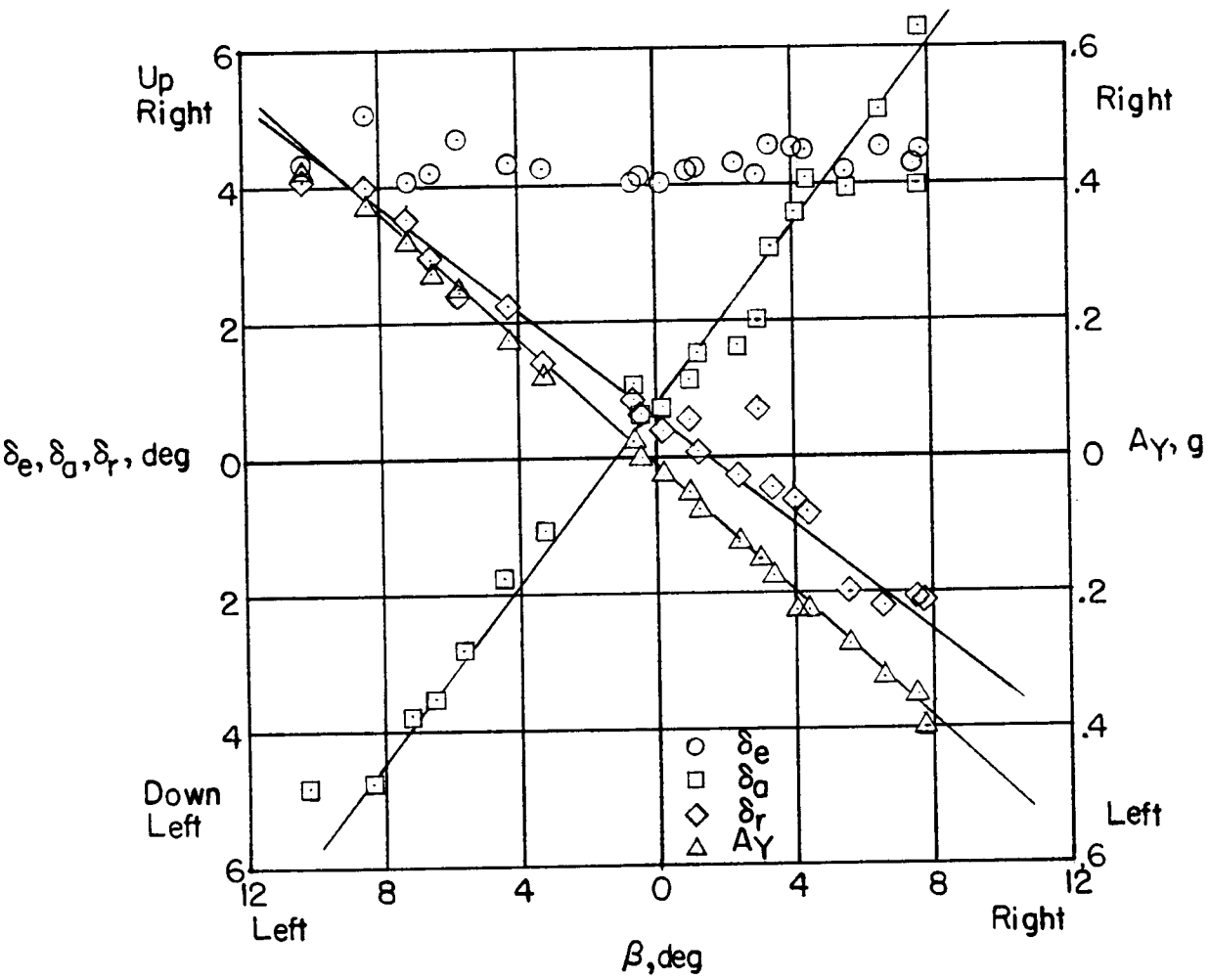

(g) V_i = 208 mph; α = 7.8°; C_{N_A} = 0.29; gear down.

Figure 4.- Continued.

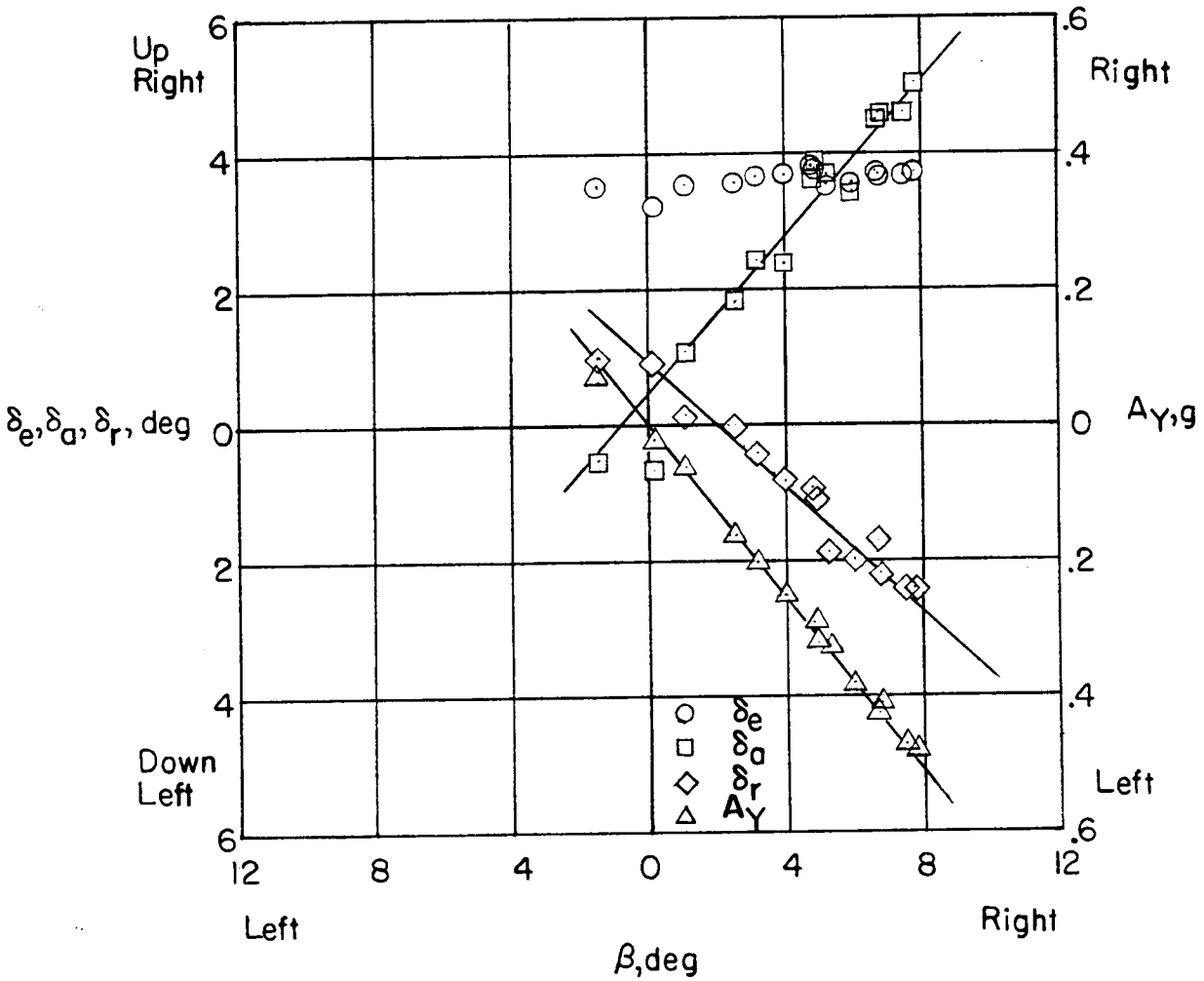

(h) V_i = 249 mph; $\alpha = 6.9^{\circ}$; C_{N_A} = 0.21; gear down.

Figure 4.- Concluded.

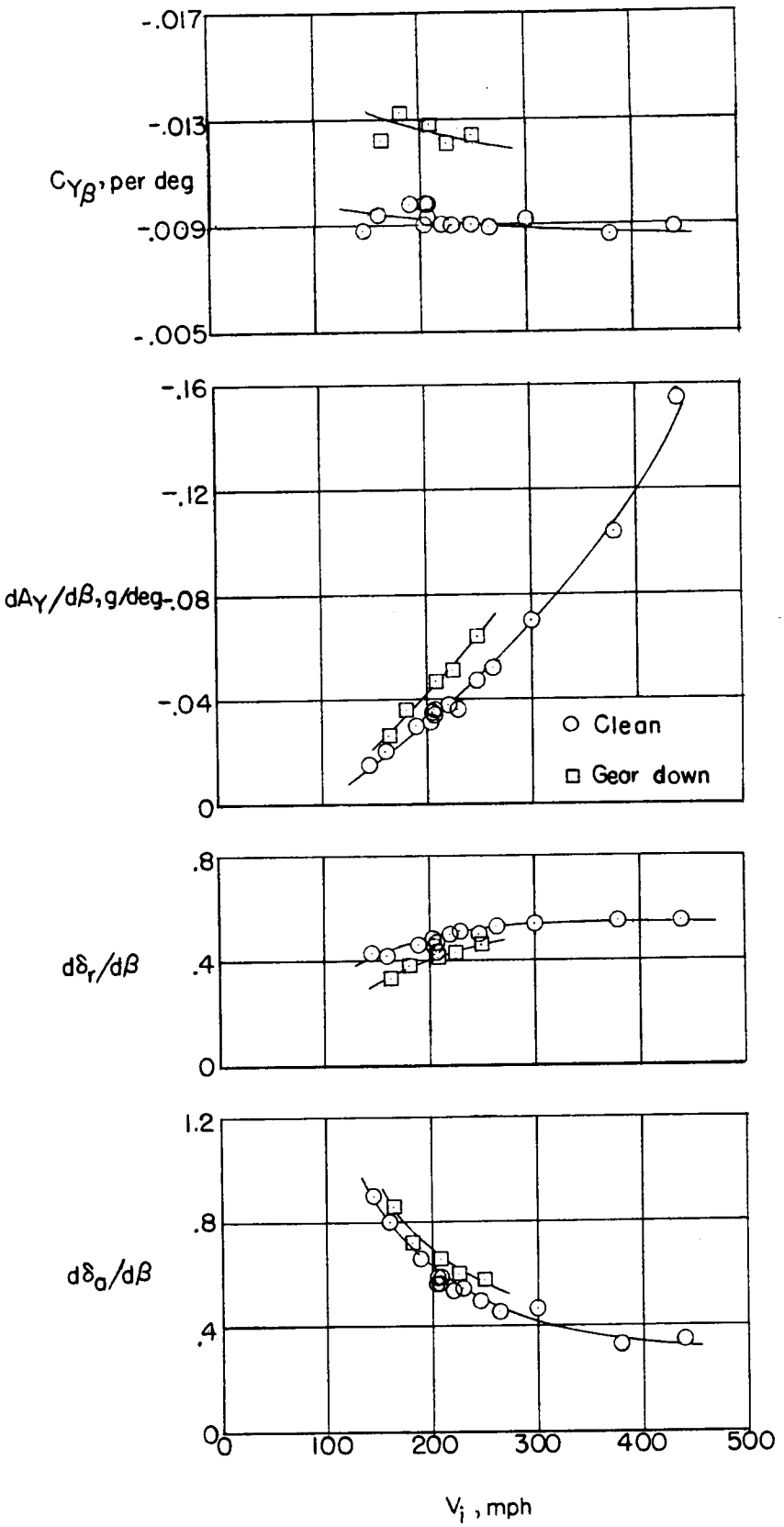

Figure 5.- Variation of lateral parameters for the basic airplane with indicated speed as determined from sideslip maneuvers.

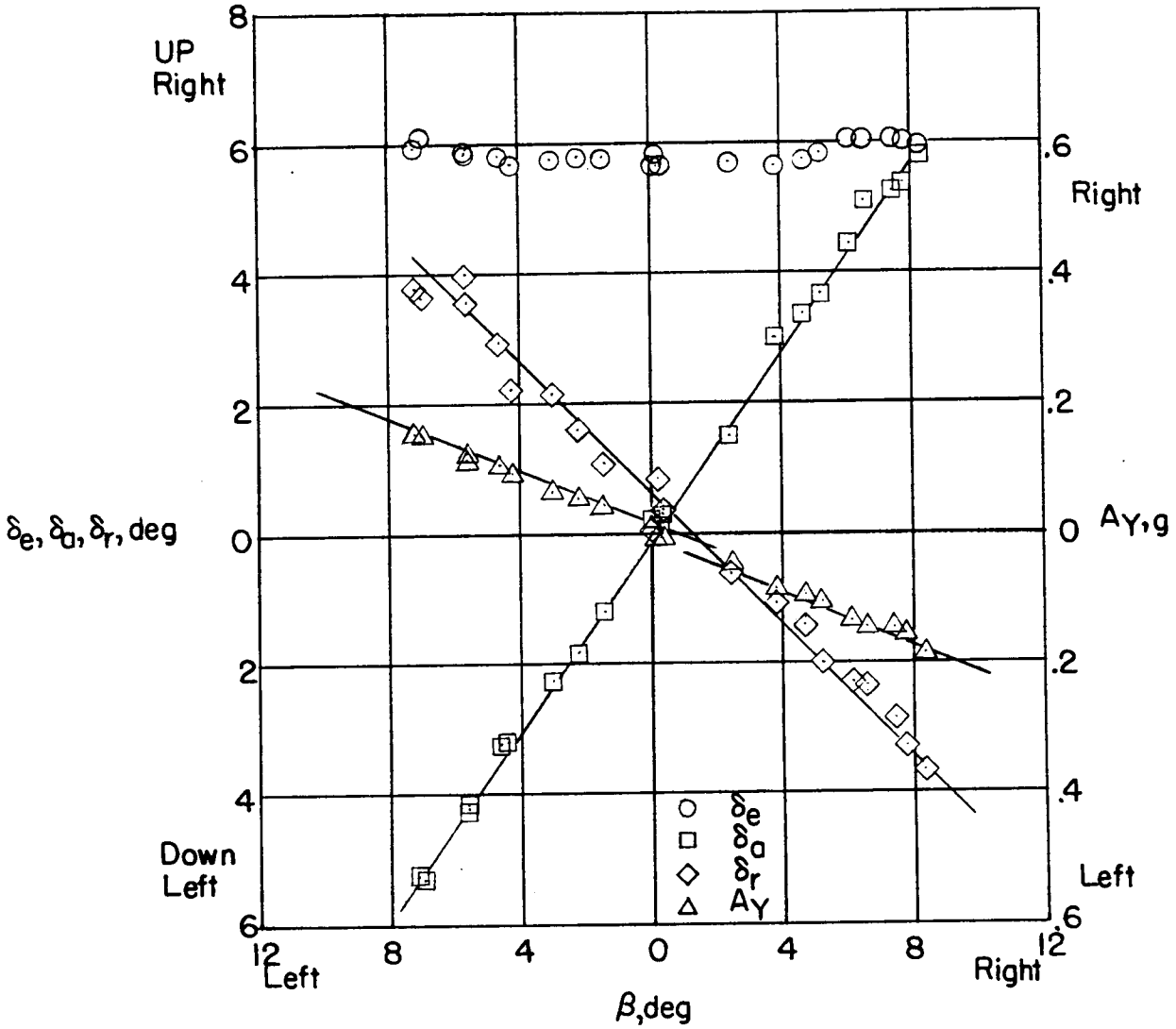

(a) V_i = 164 mph; α = 14.4°; C_{N_A} = 0.49; clean.

Figure 6.- Variation of control positions and transverse acceleration factor with angle of sideslip for the fence configuration.

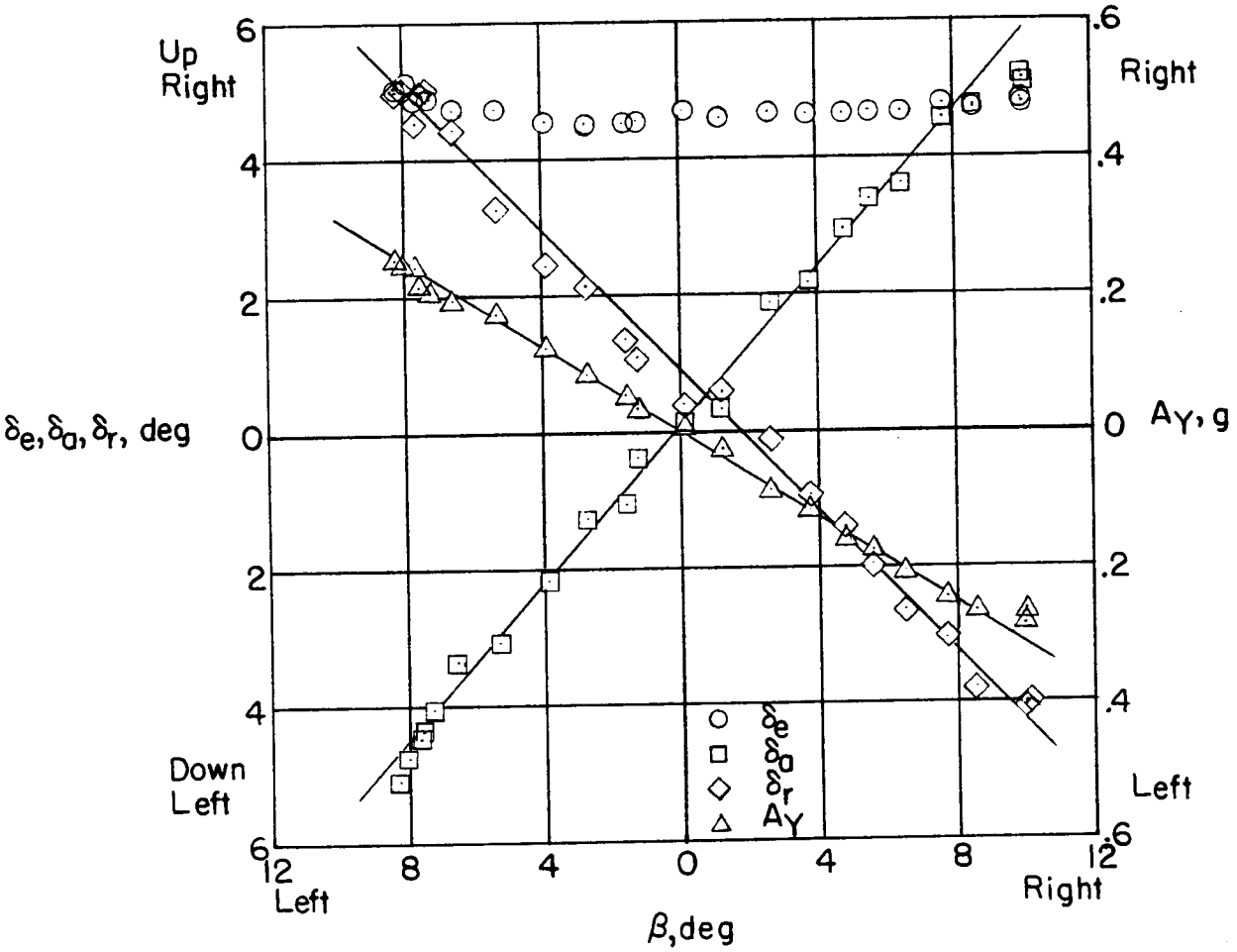

(b) V_i = 204 mph; α = 9.9°; C_{N_A} = 0.32; clean.

Figure 6.- Continued.

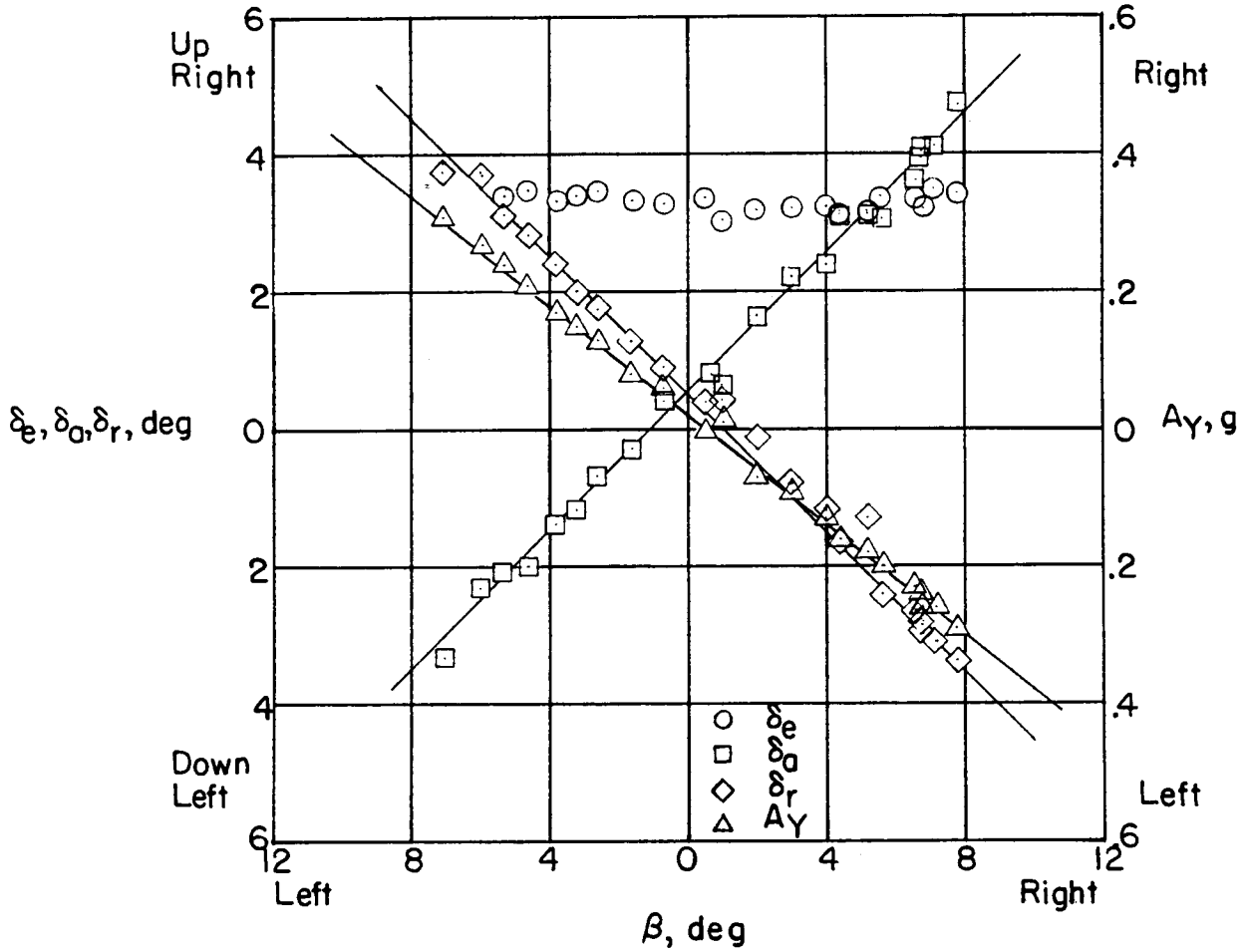

(c) V_i = 226 mph; α = 7.4°; C_{N_A} = 0.26; clean.

Figure 6.- Continued.

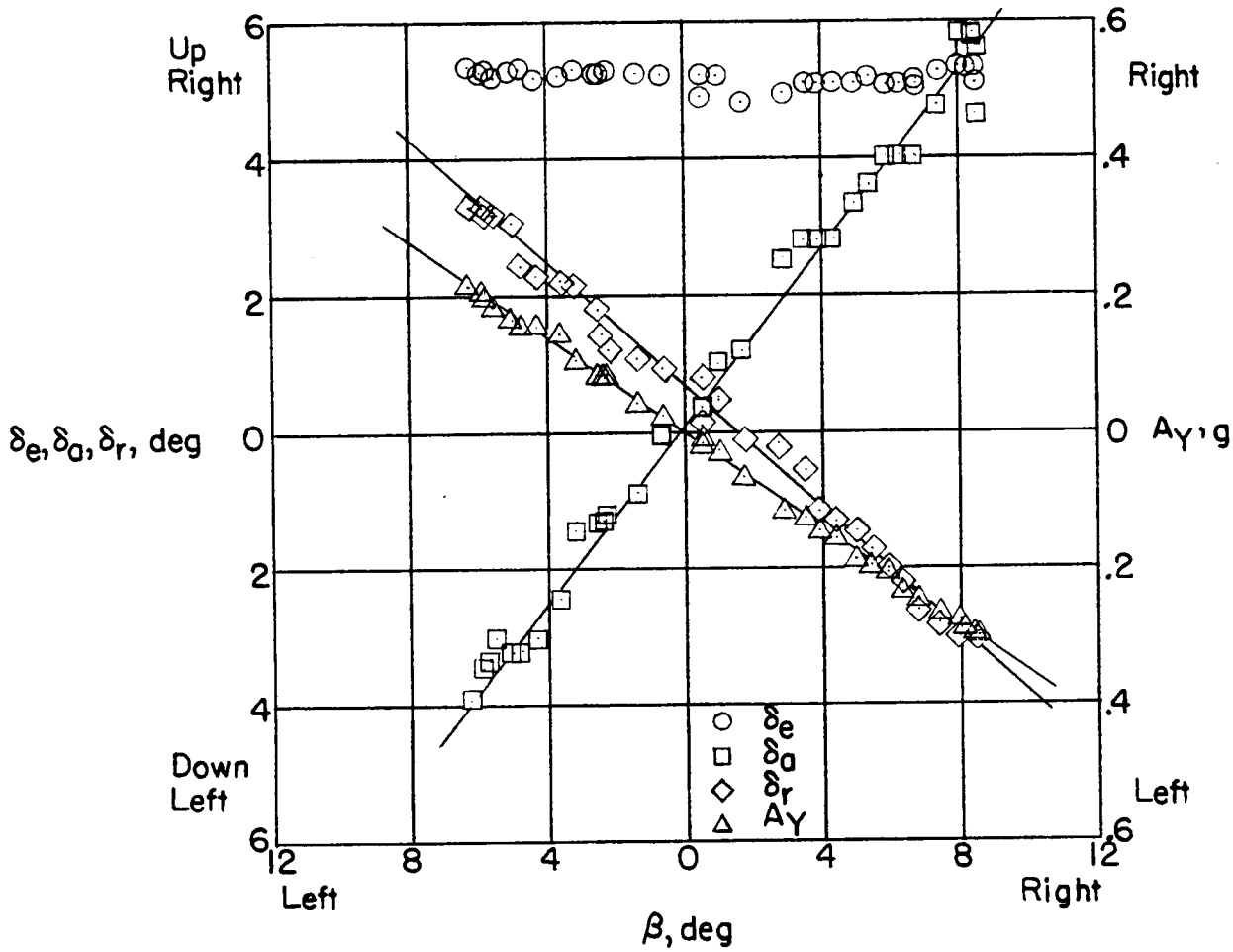

(d) V_i = 186 mph; α = 11.0°; C_{N_A} = 0.37; gear down.

Figure 6.- Continued.

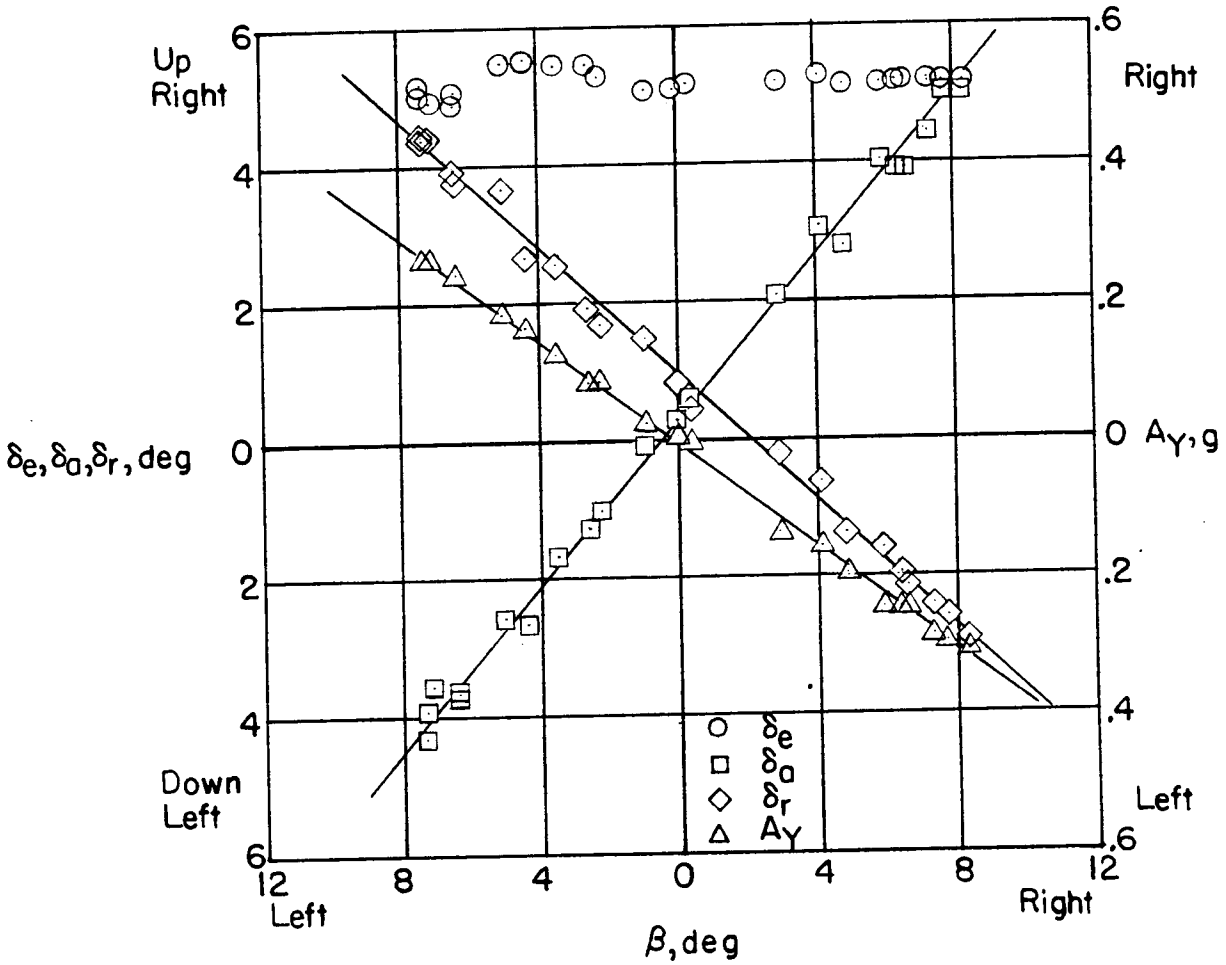

(e) V_i = 205 mph; α = 10.4°; C_{N_A} = 0.34; gear down.

Figure 6.- Continued.

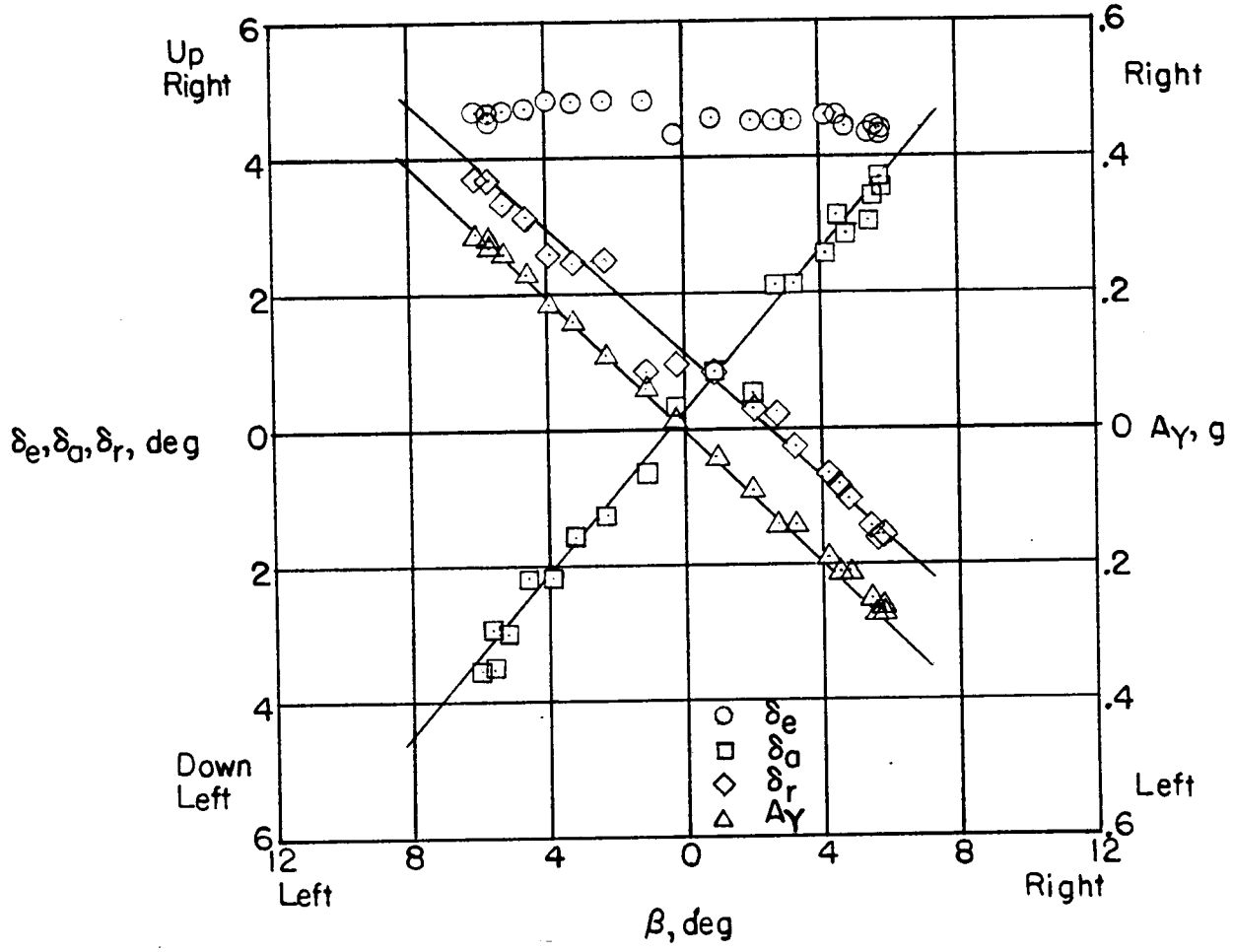

(f) V_i = 225 mph; α = 8.1°; C_{N_A} = 0.27; gear down.

Figure 6.- Concluded.

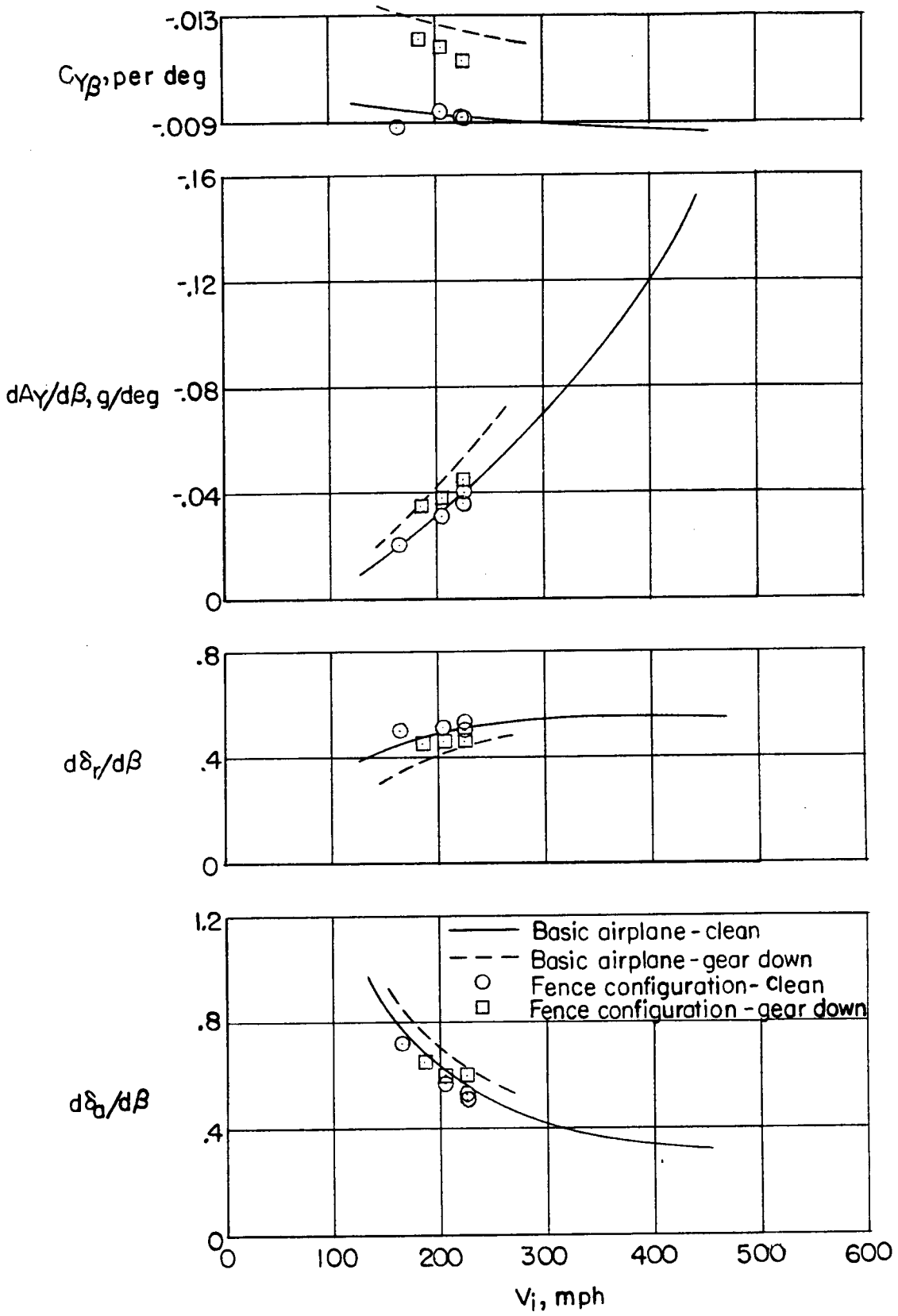

Figure 7.- Variation of lateral parameters for the fence configuration with indicated speed as determined from sideslip maneuvers.

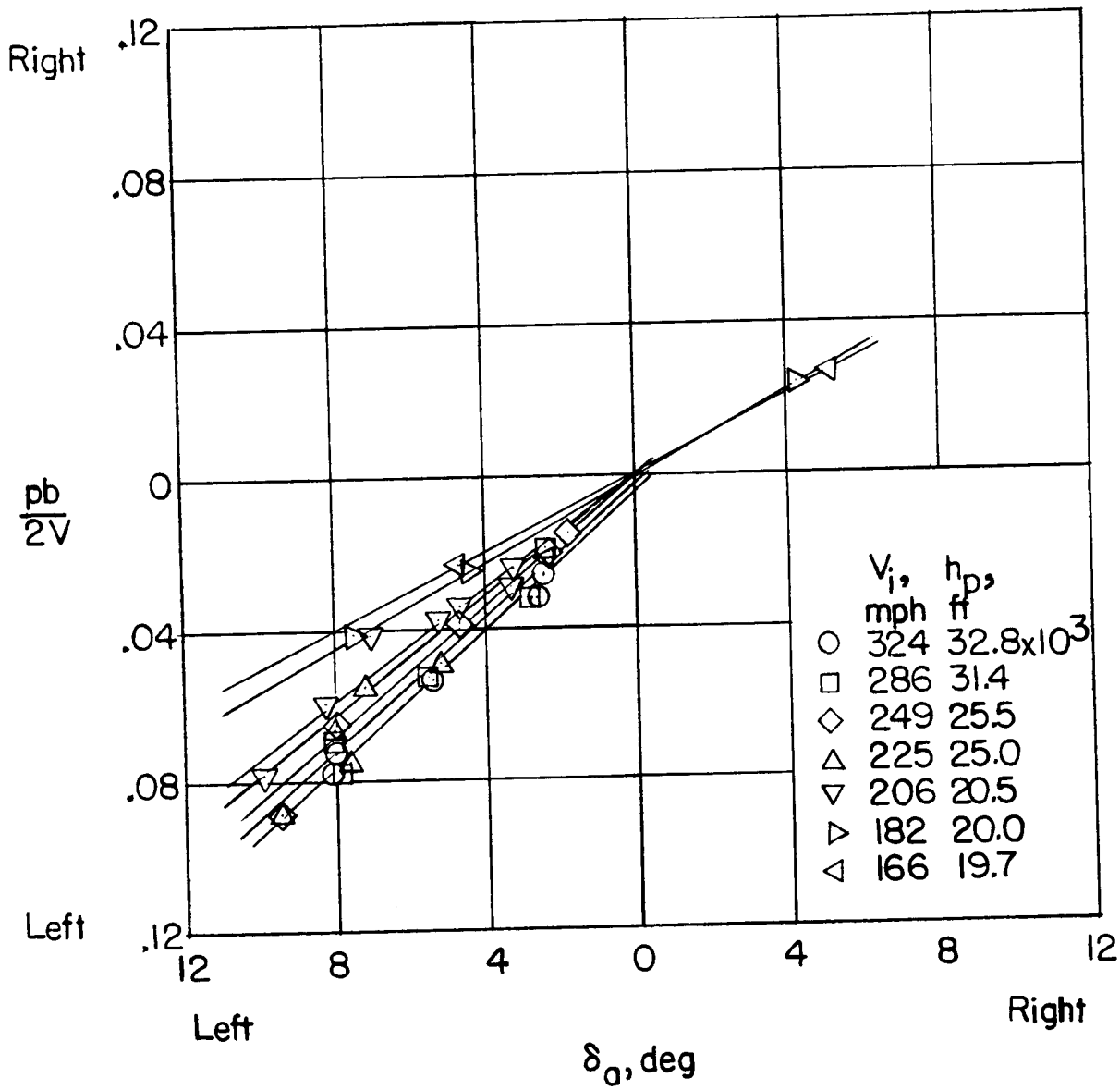

(a) Basic airplane; clean.

Figure 8.- Variation of wing-tip helix angle with lateral control angle for the basic airplane.

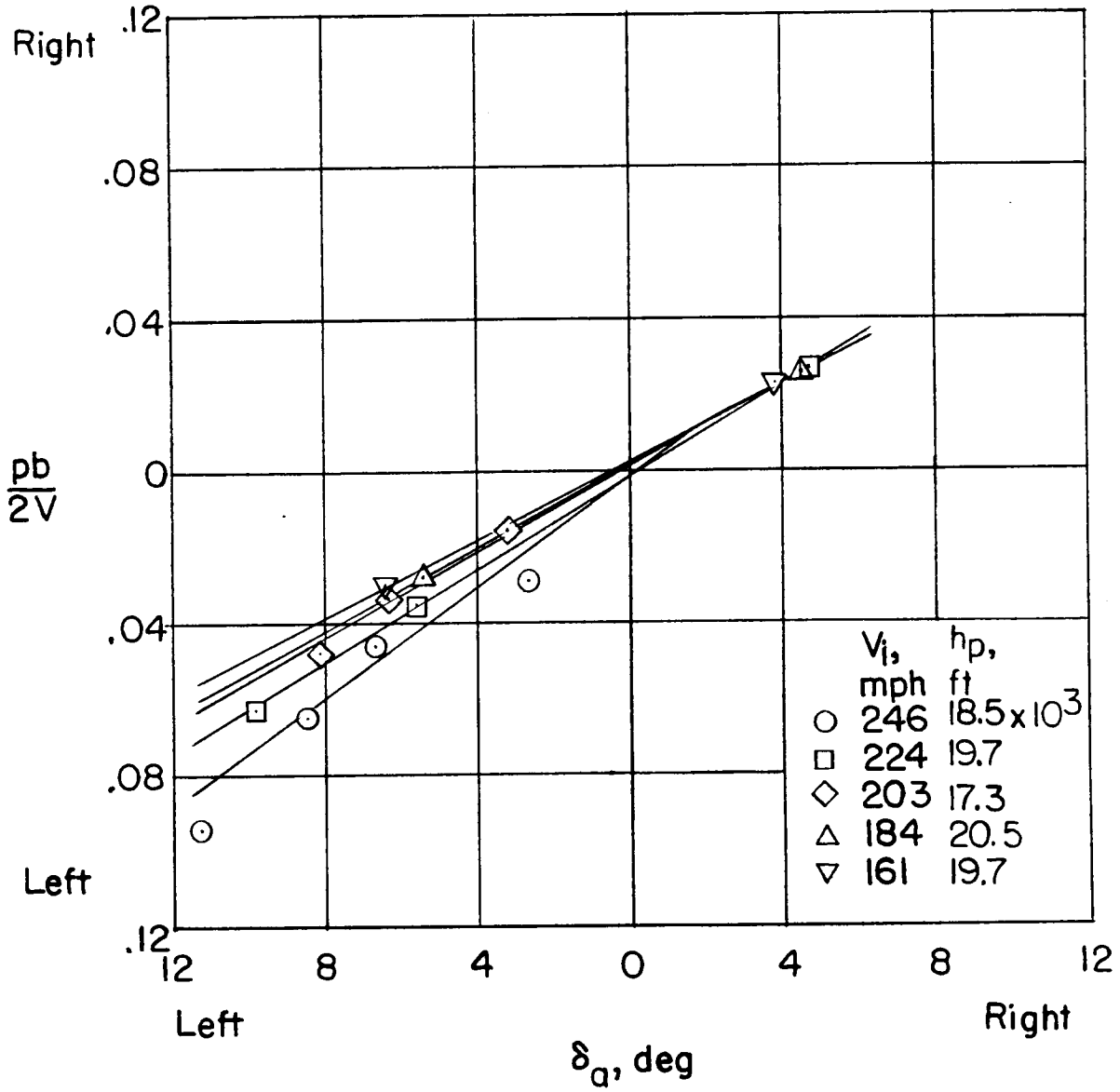

(b) Basic airplane; gear down.

Figure 8.- Concluded.

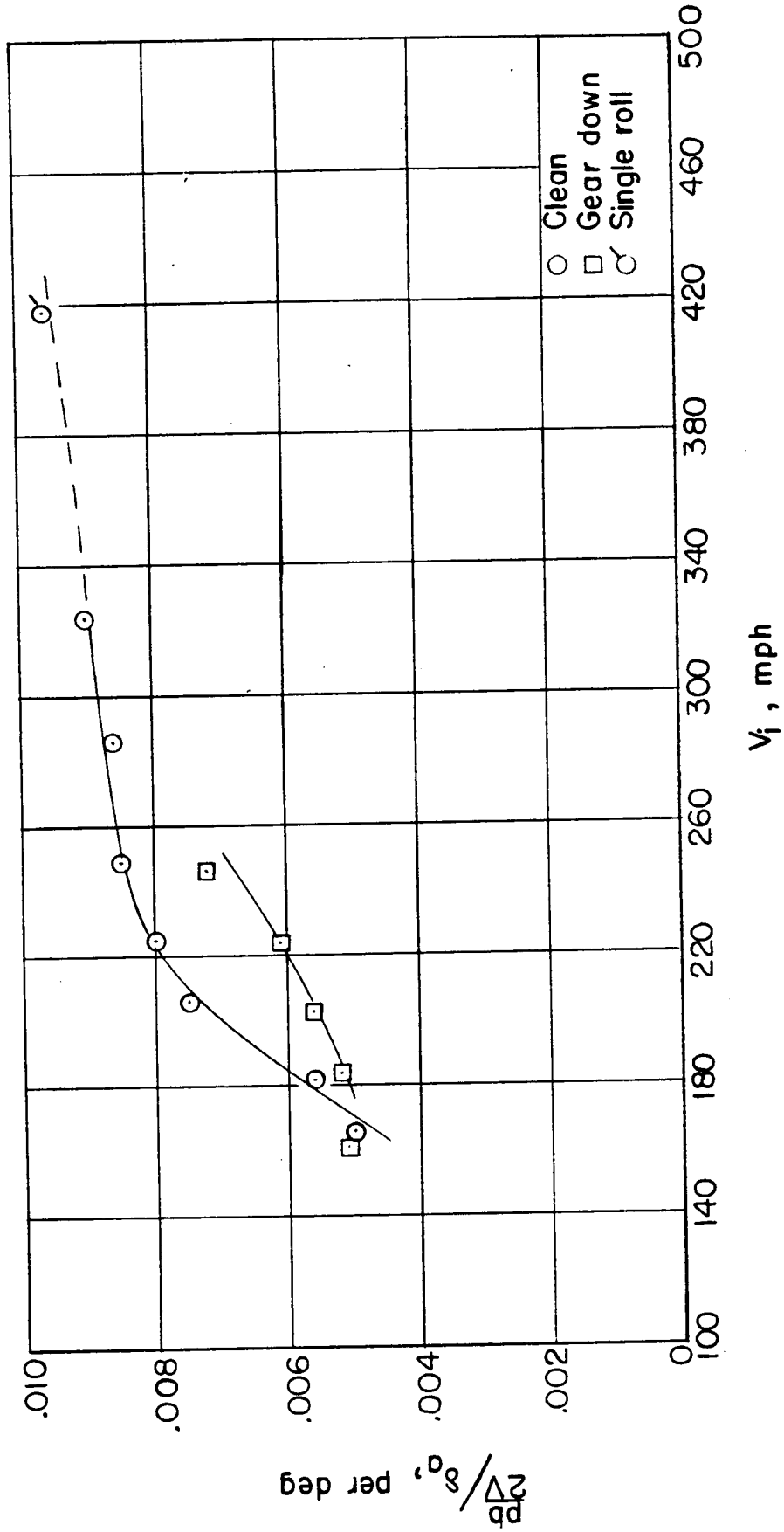

Figure 9.- Variation of helix angle per degree lateral control angle with indicated speed for the basic airplane clean and gear down.

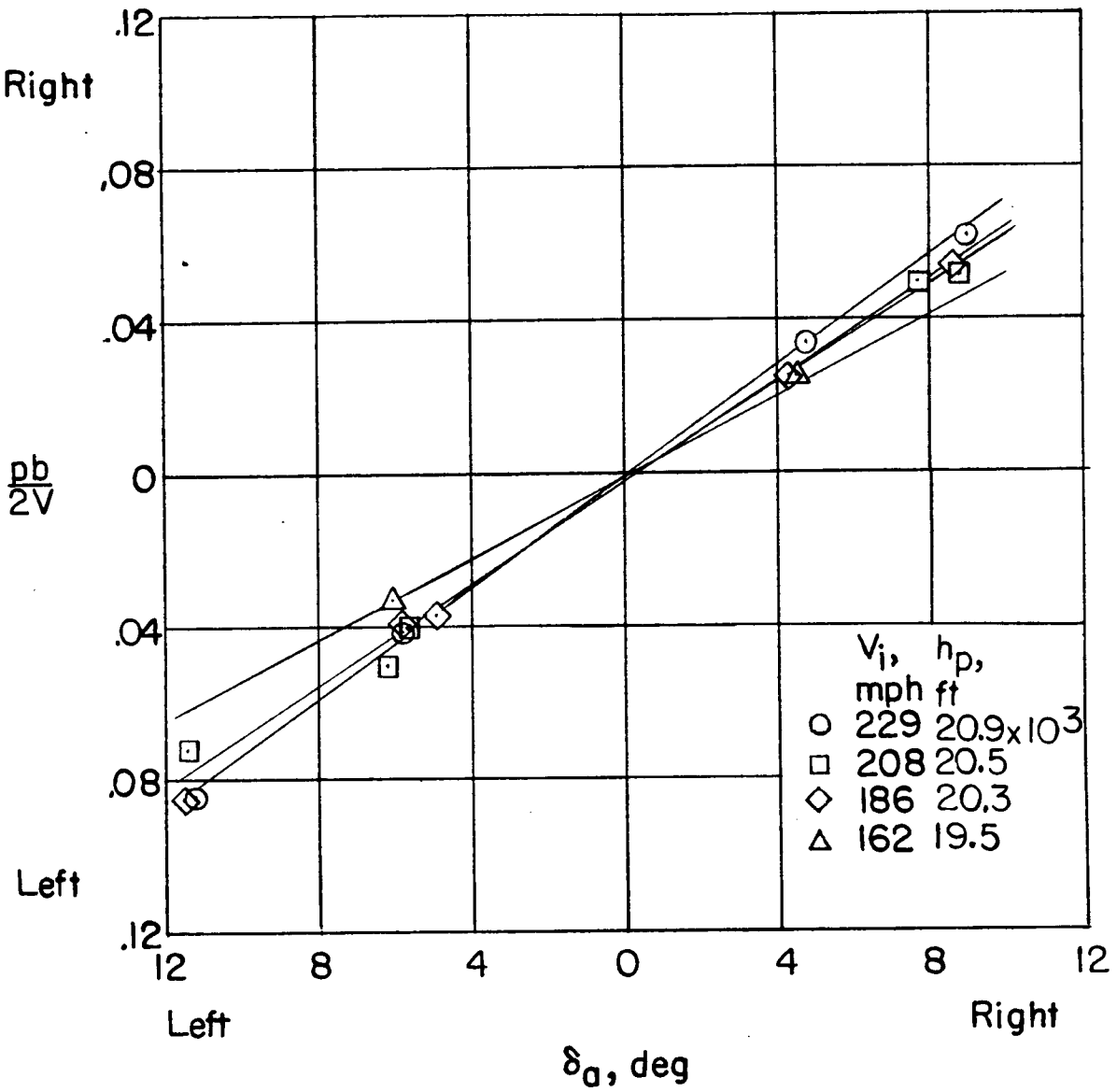

(a) Fence configuration; clean.

Figure 10.- Variation of wing-tip helix angle with lateral control angle for the fence configuration.

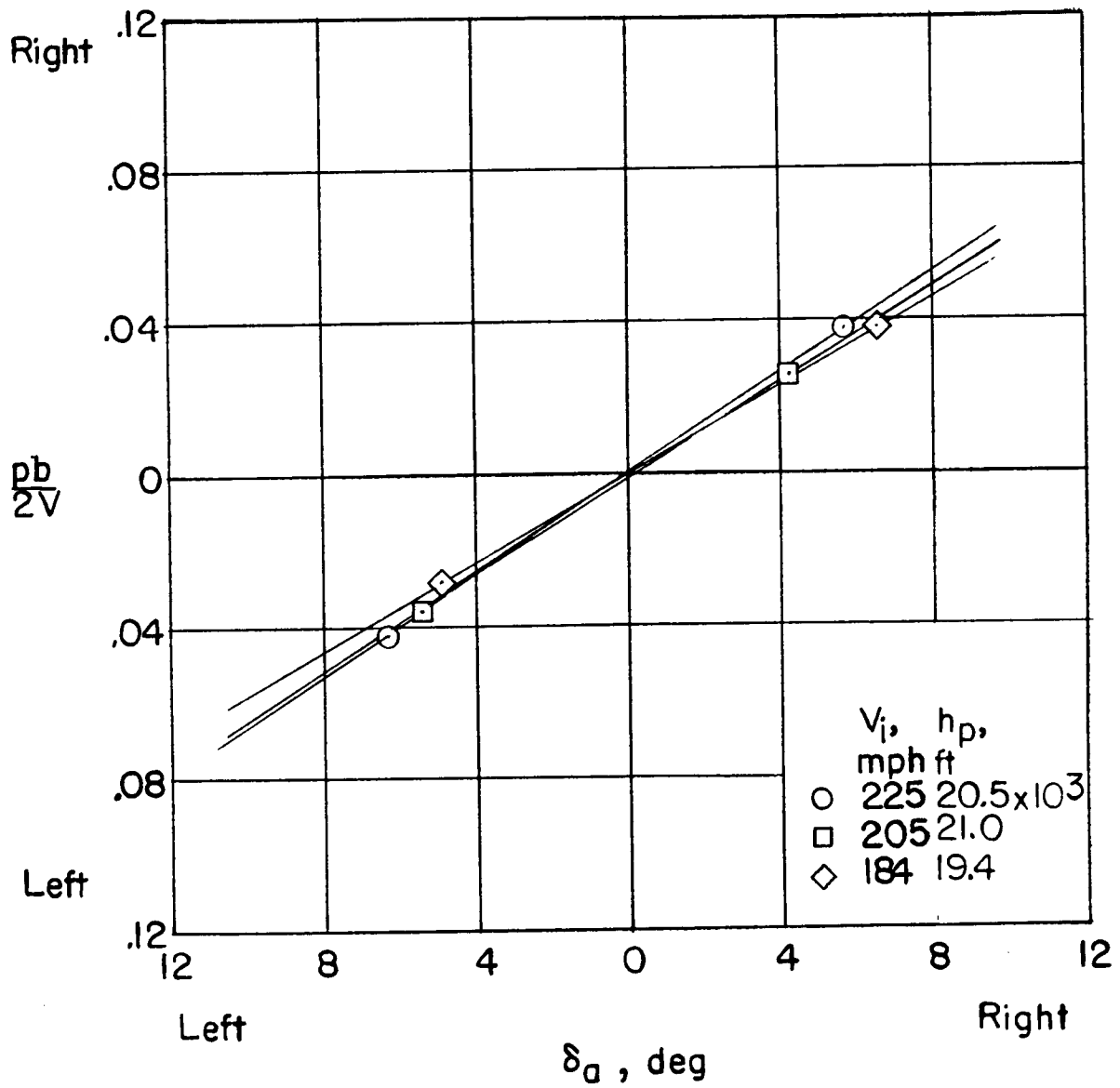

(b) Fence configuration; gear down.

Figure 10.- Concluded.

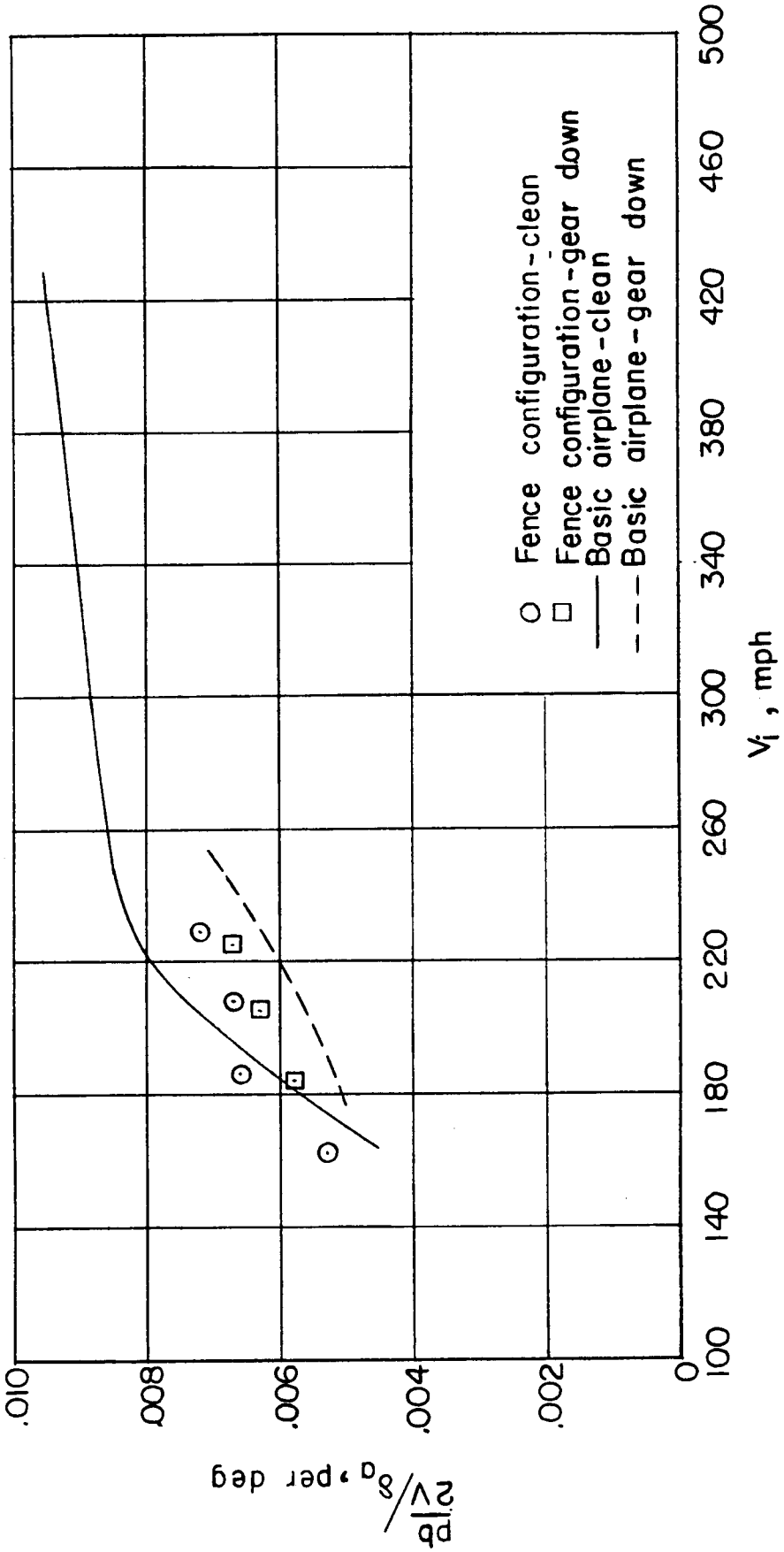

Figure 11.- Variation of helix angle per degree lateral control angle with indicated speed for the fence configuration clean and gear down.

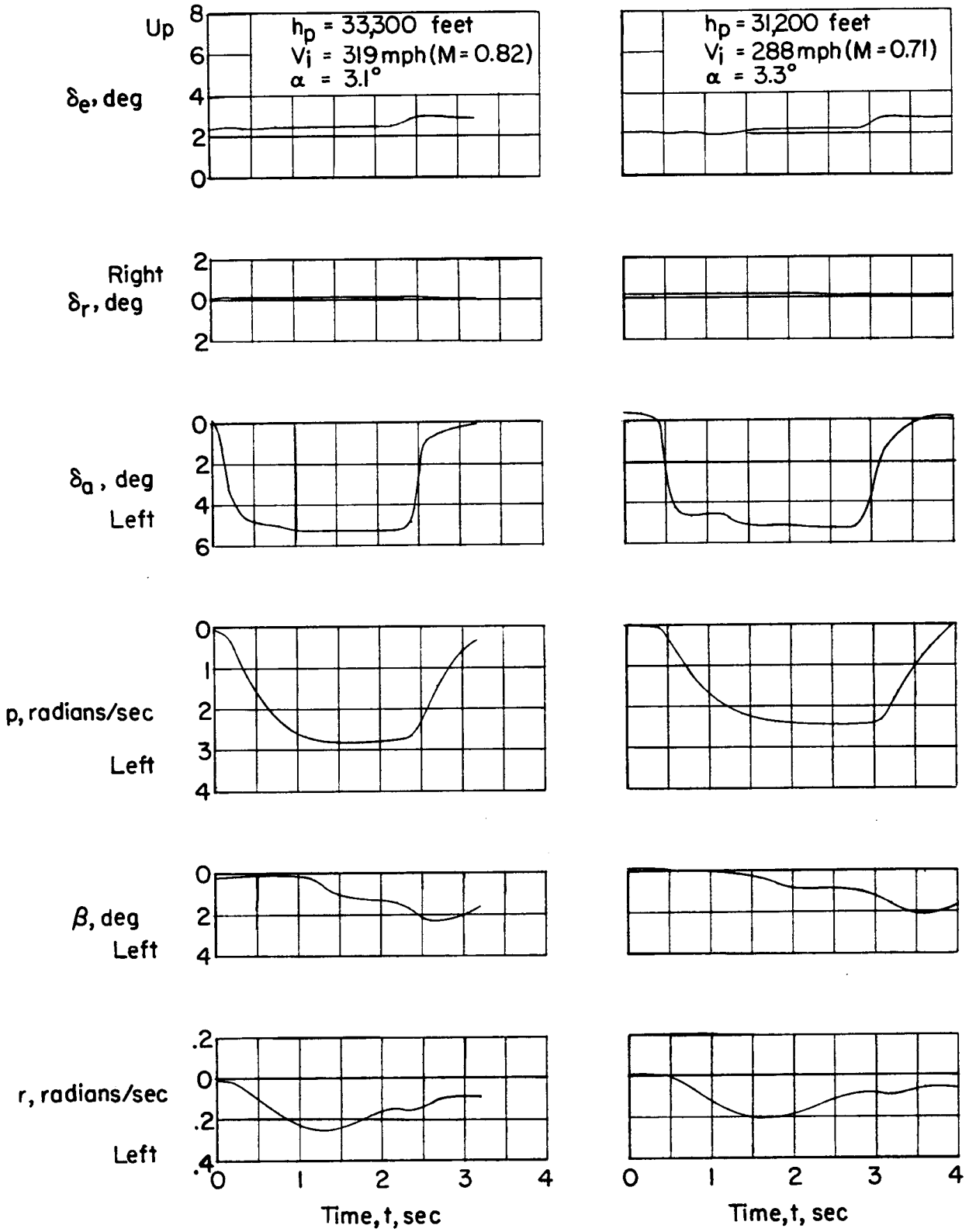

(a) Basic airplane; clean. (b) Basic airplane; clean.

Figure 12.- Representative time histories of rudder-fixed aileron rolls.

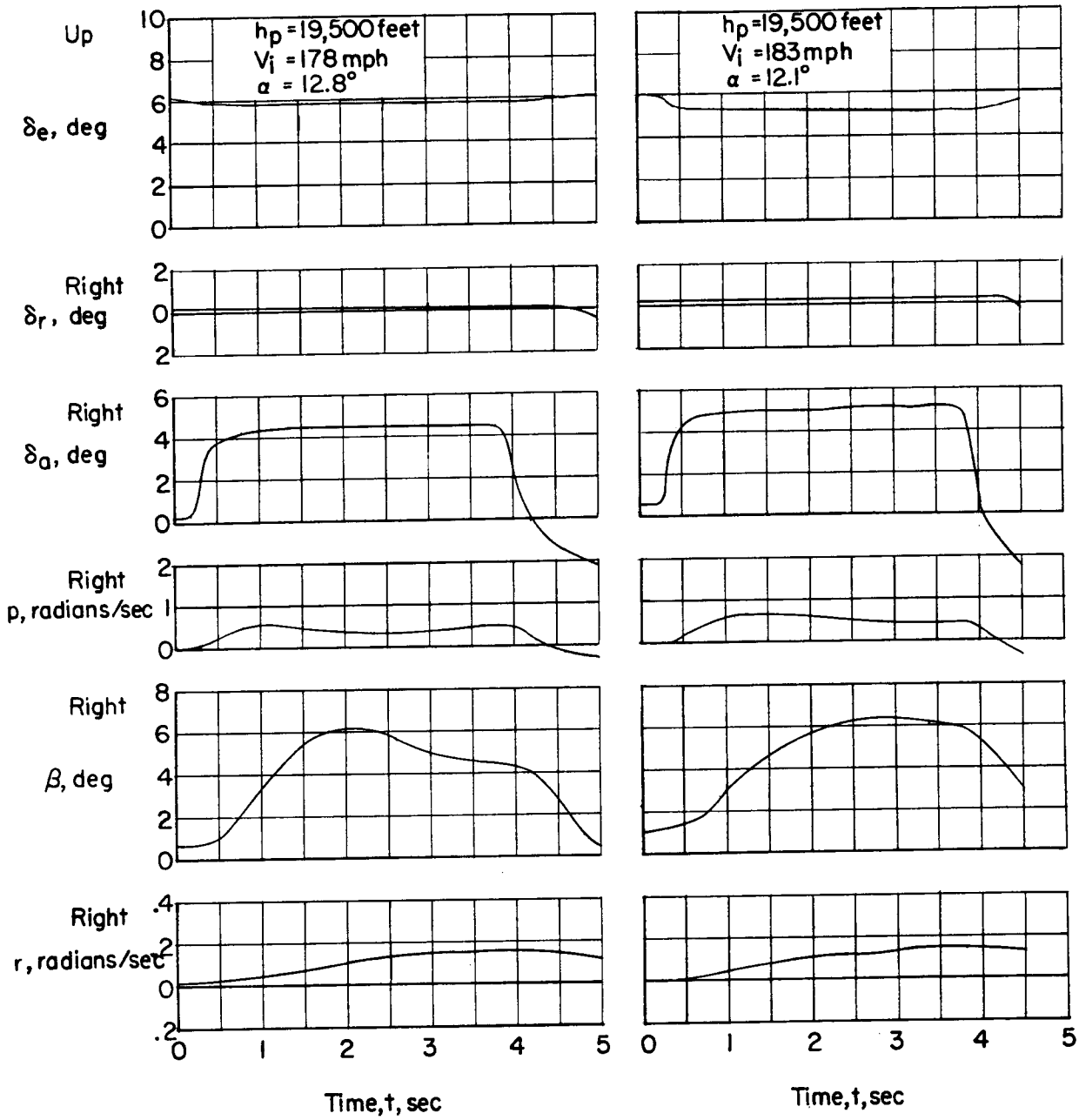

(c) Basic airplane; clean. (d) Basic airplane; gear down.

Figure 12.- Continued.

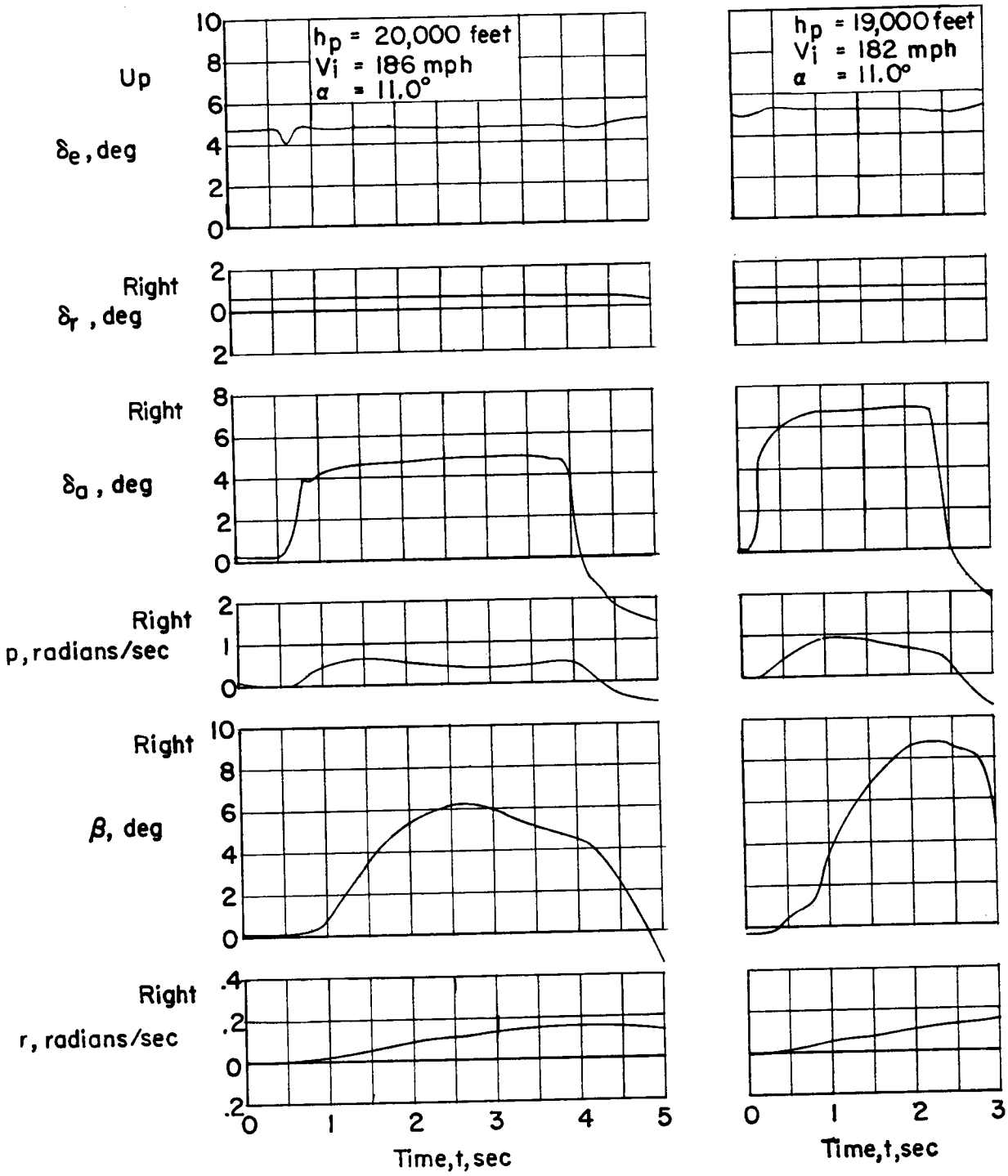

(e) Fence configuration; clean. (f) Fence configuration; gear down.

Figure 12.- Concluded.

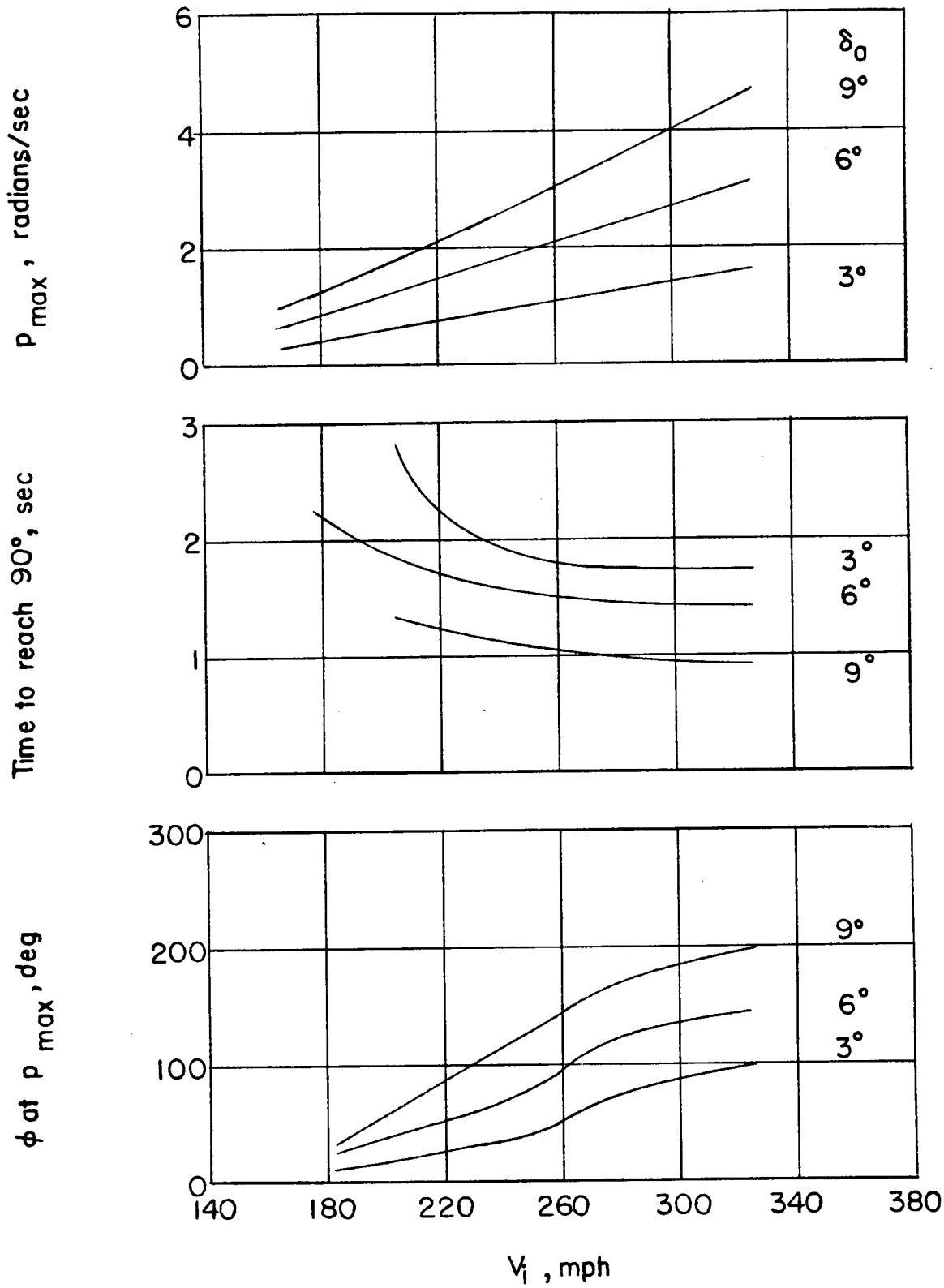

(a) Basic airplane; clean.

Figure 13.- Variation of rolling effectiveness with indicated speed.

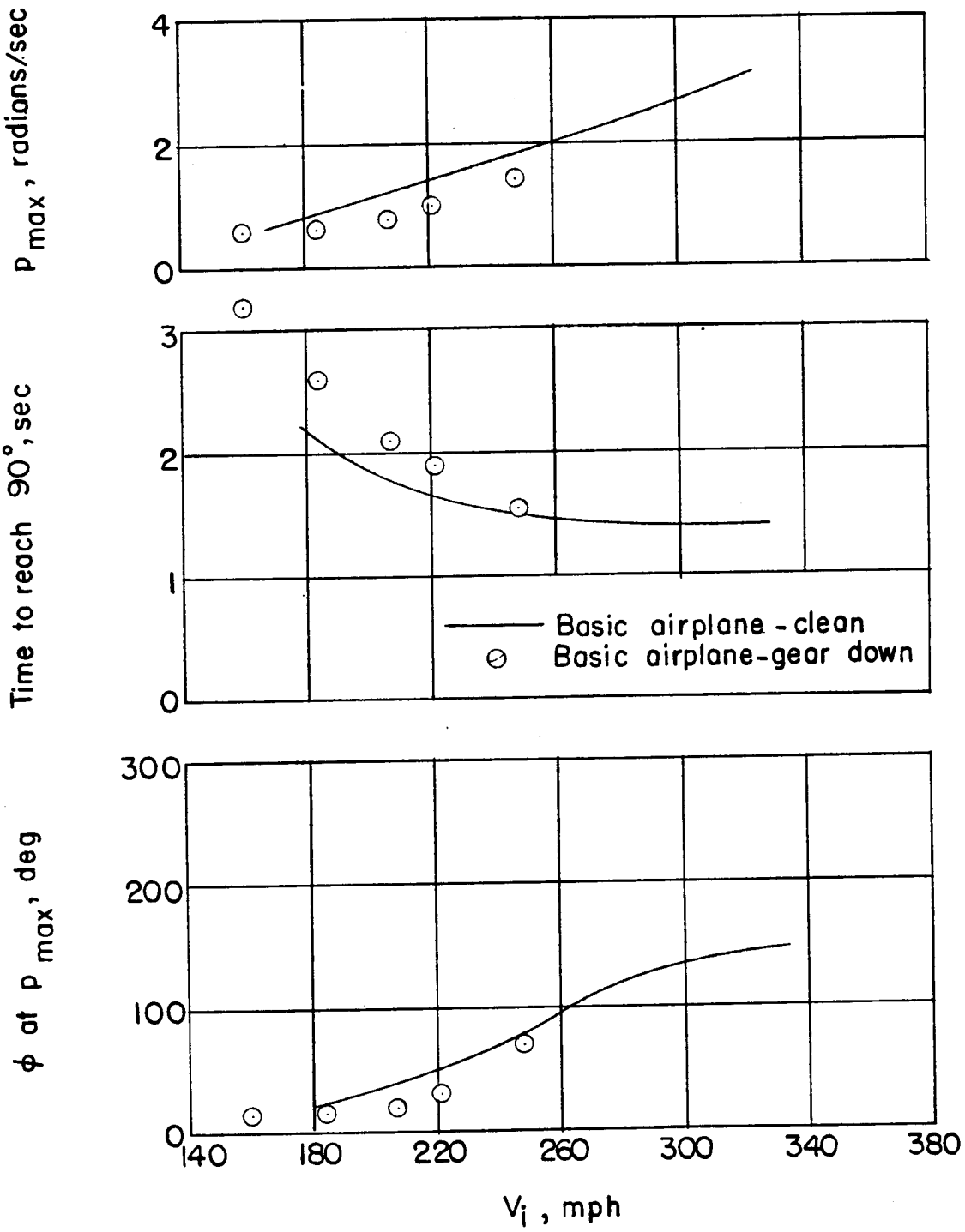

(b) Basic airplane; gear down; $\delta_a \approx 6^{\circ}$.

Figure 13.- Continued.

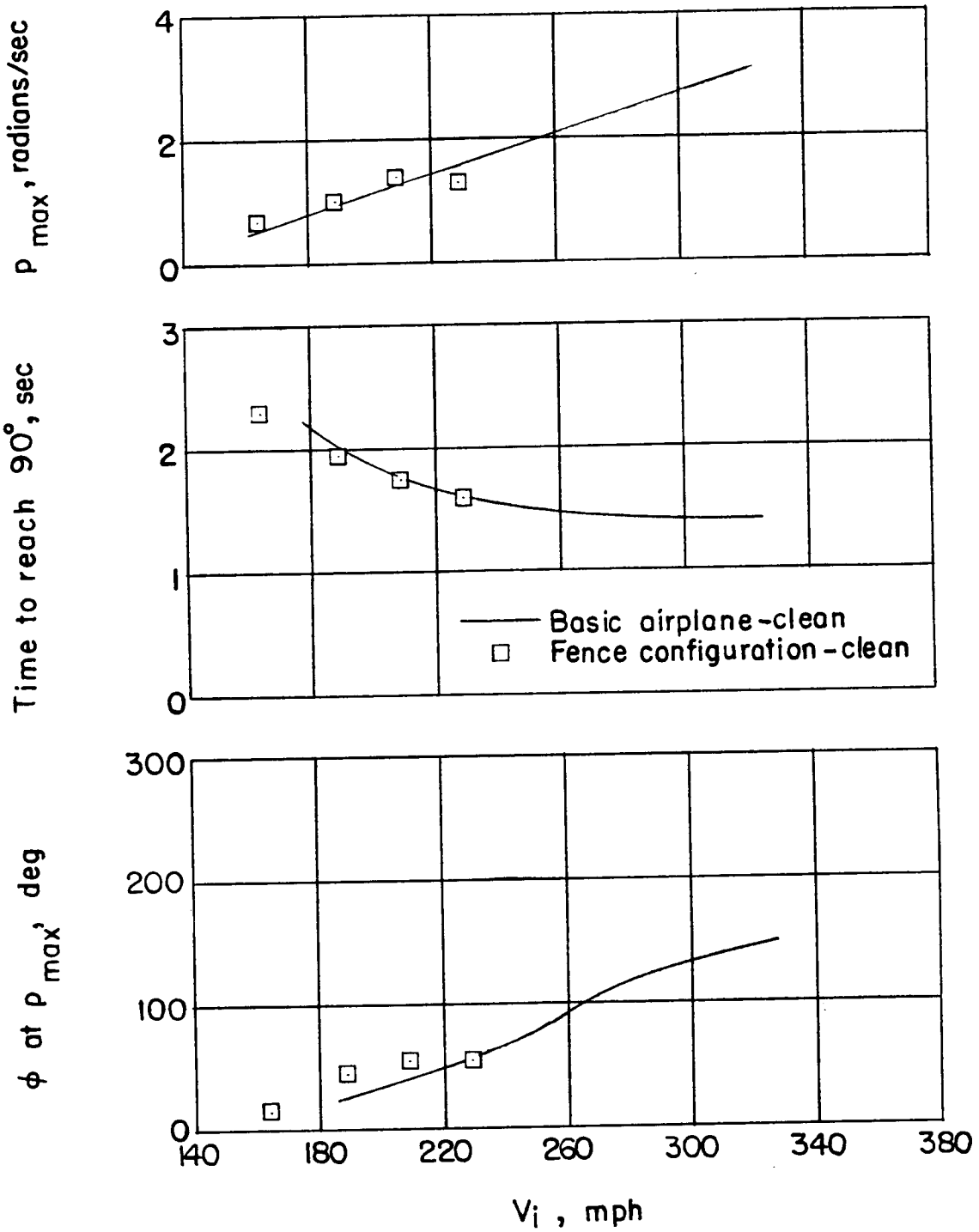

(c) Fence configuration; clean; $\delta_a \approx 6^\circ$.

Figure 13.- Continued.

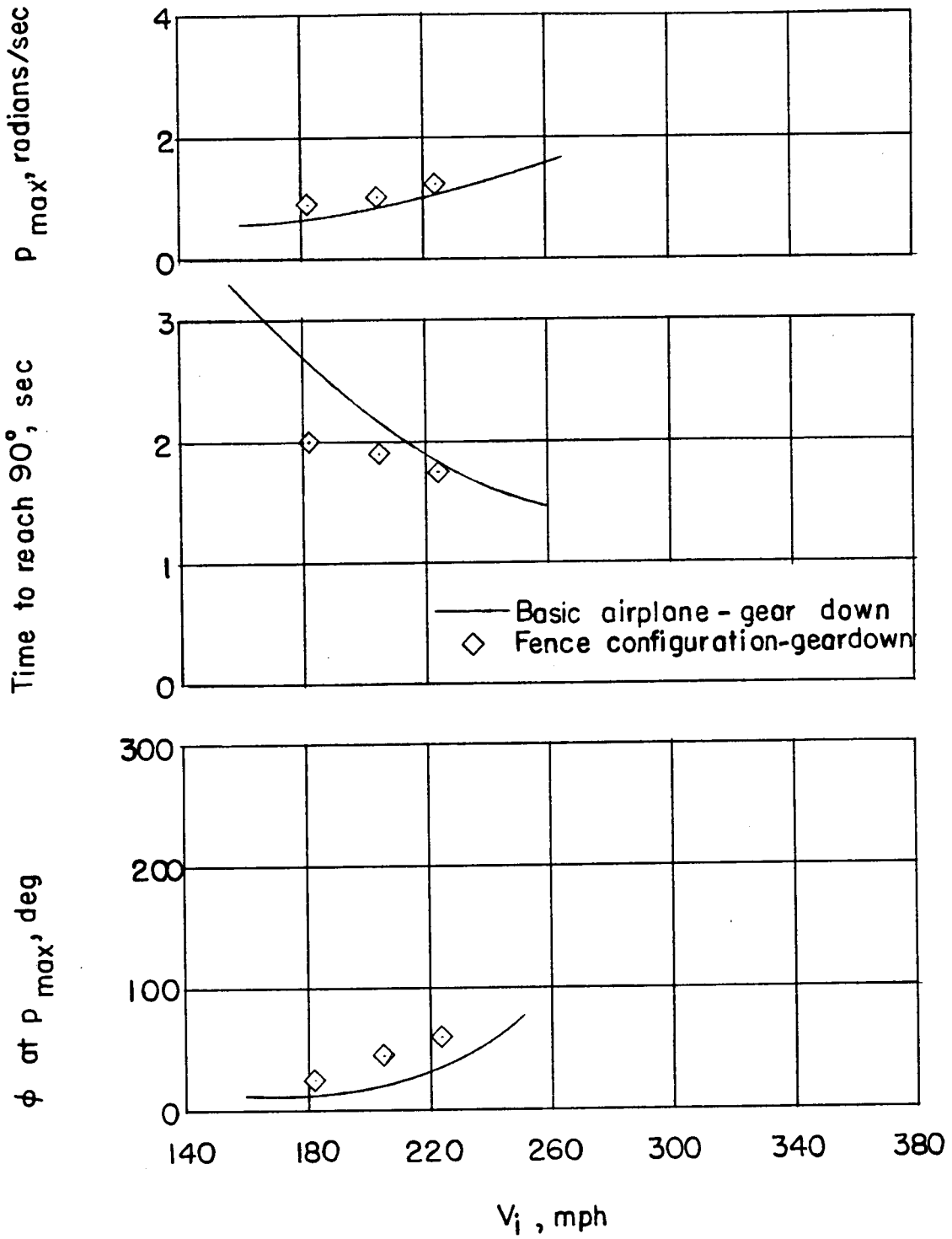

(d) Fence configuration; gear down; $\delta_a \approx 6^{\circ}$.

Figure 13.- Concluded.

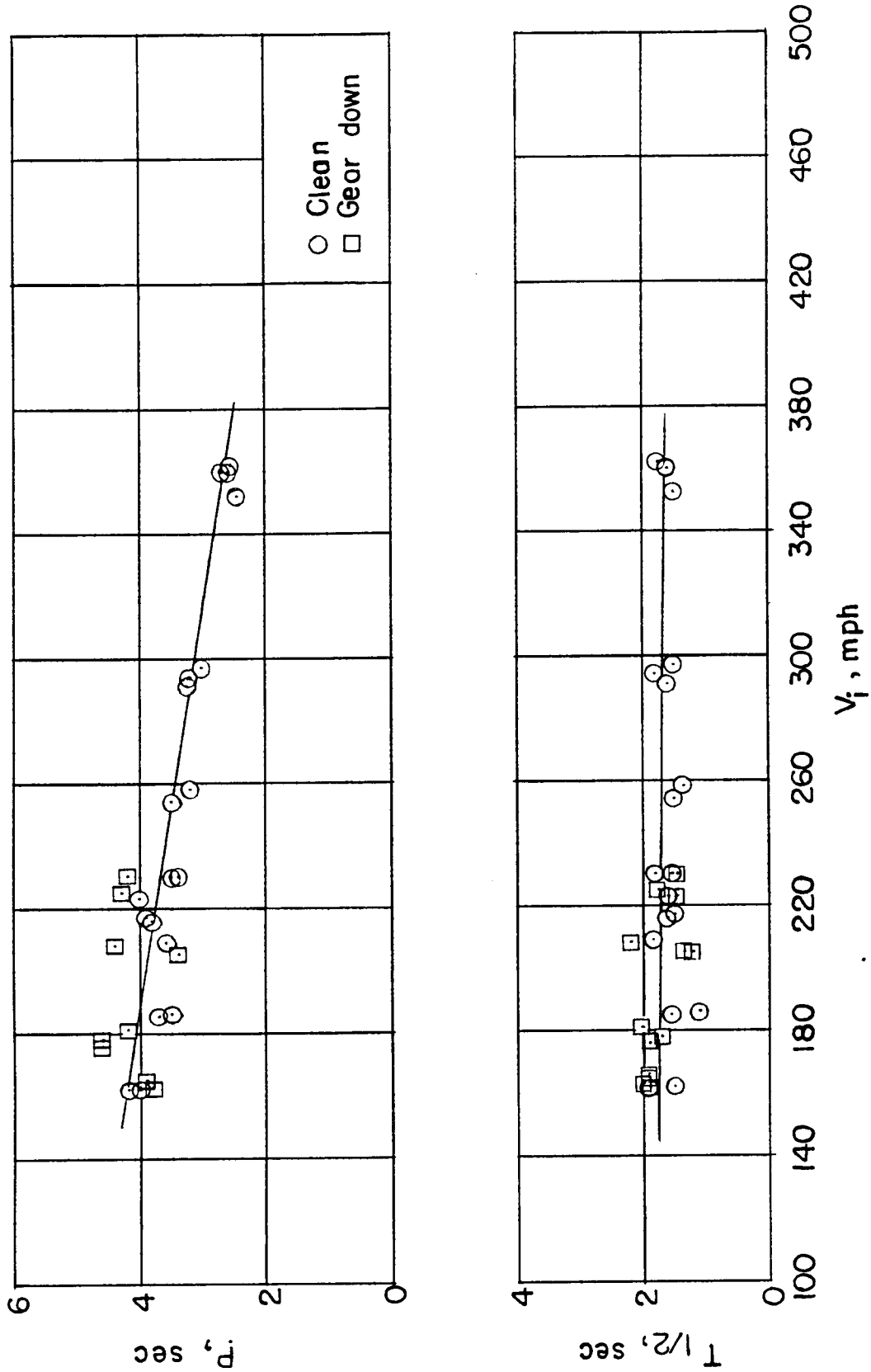

(a) Basic airplane.

Figure 14.- Variation of period and damping with indicated speed. h_p = 20,000 feet.

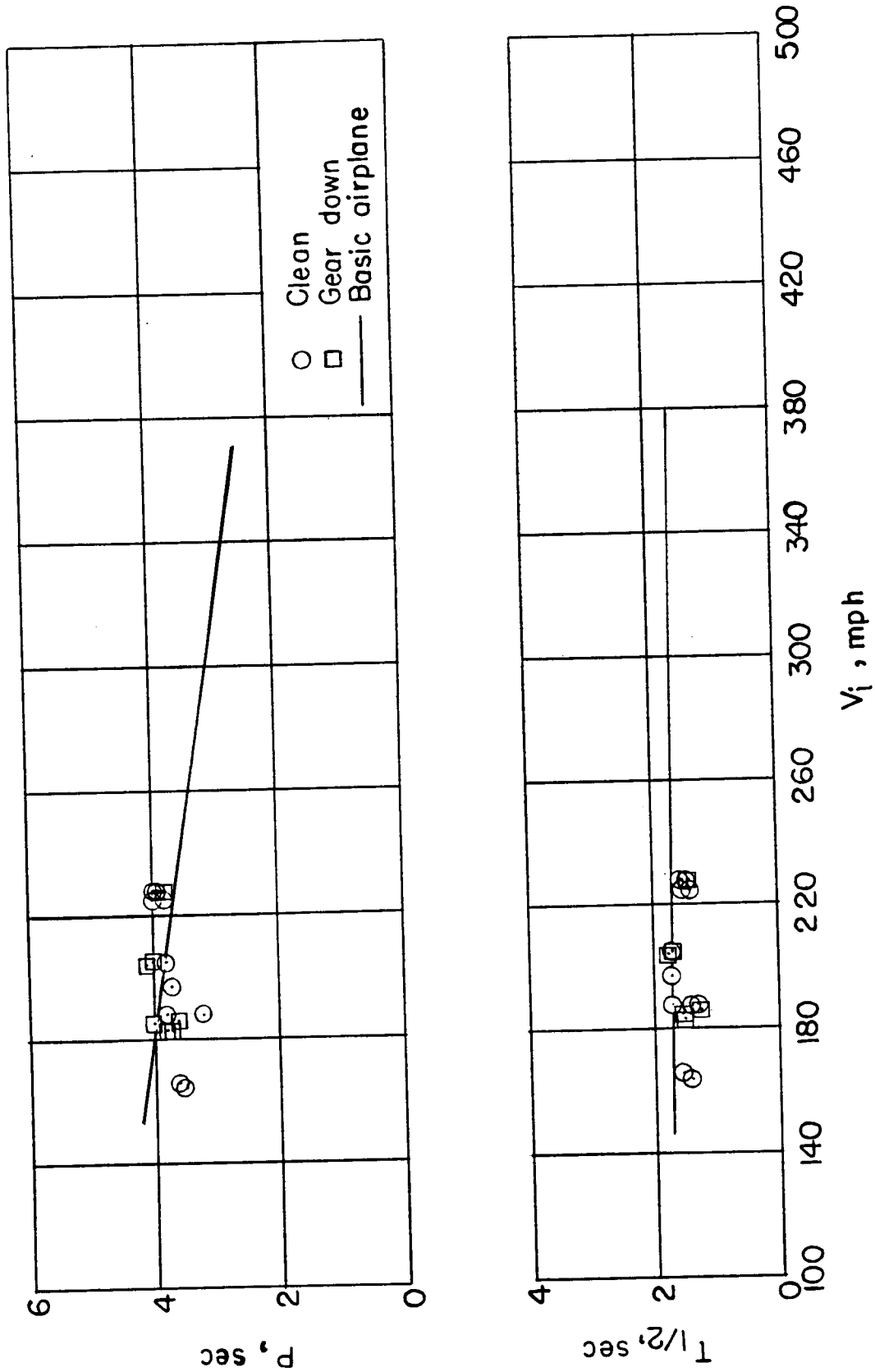

(b) Fence configuration.

Figure 14.- Concluded.

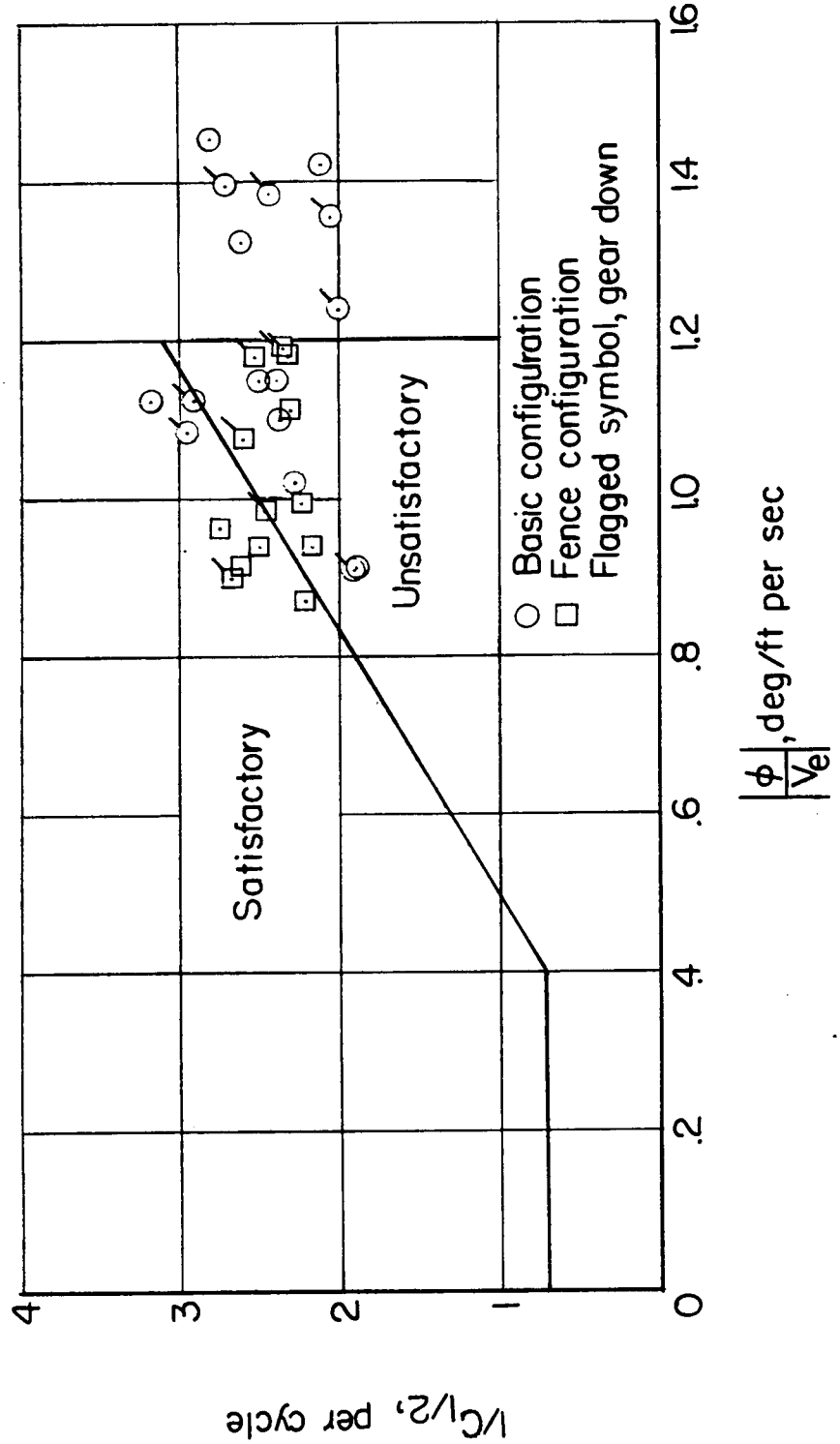

Figure 15.- Comparison of the dynamic lateral stability with the requirement of reference 8.

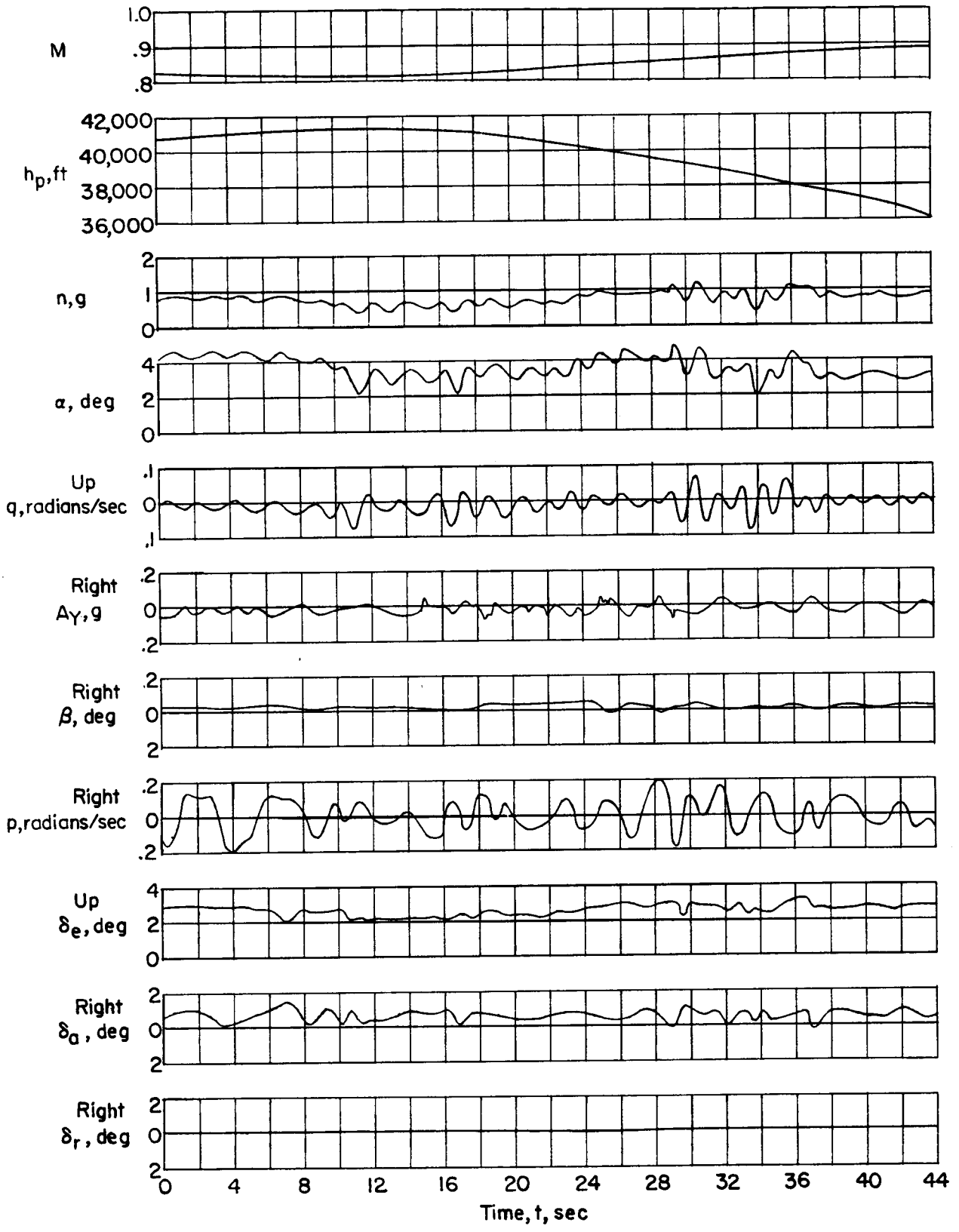

Figure 16.- Time history of high-speed trim run.

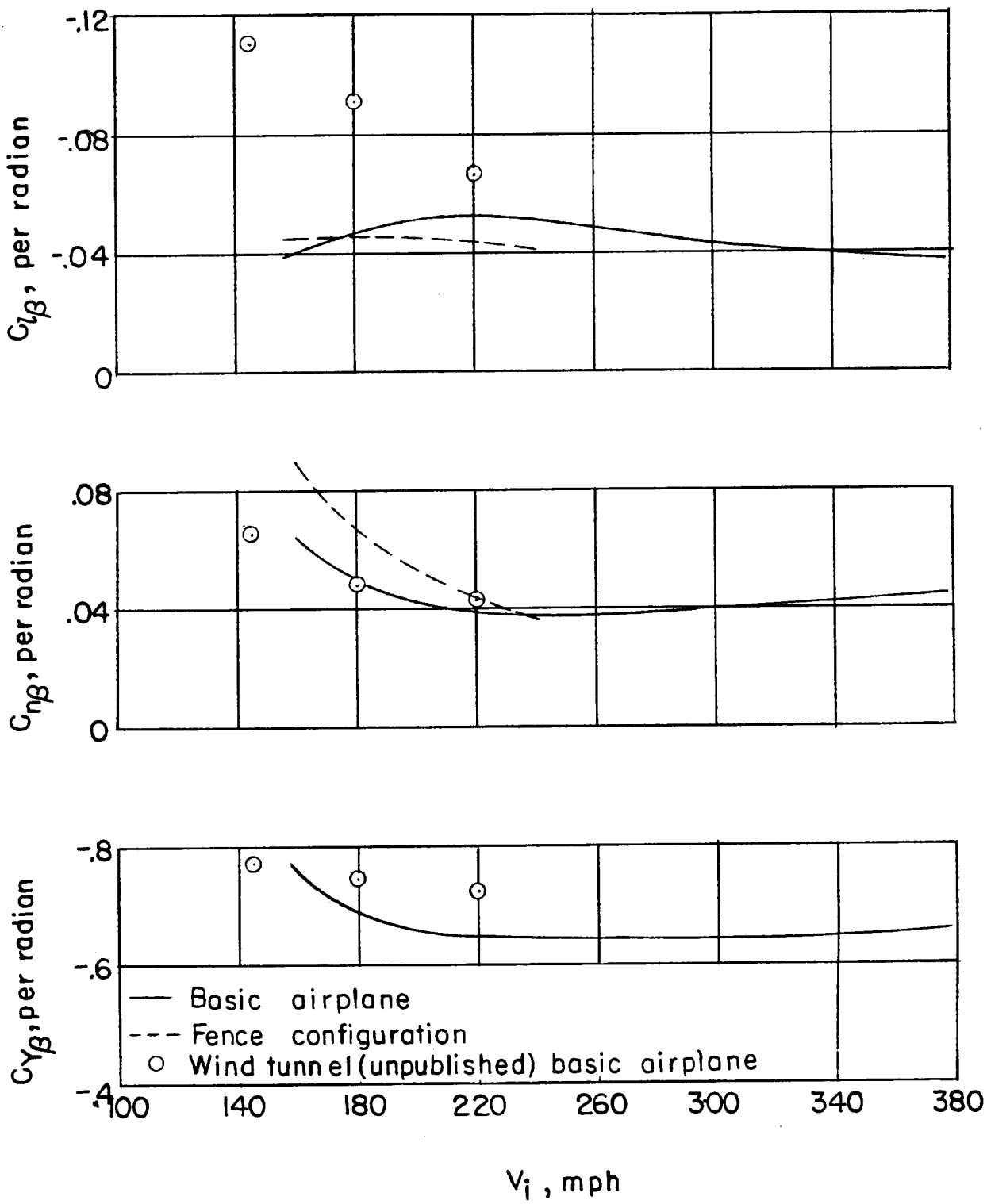

Figure 17.- Variation of lateral stability derivatives with indicated speed from flight data. h_p = 20,000 feet.

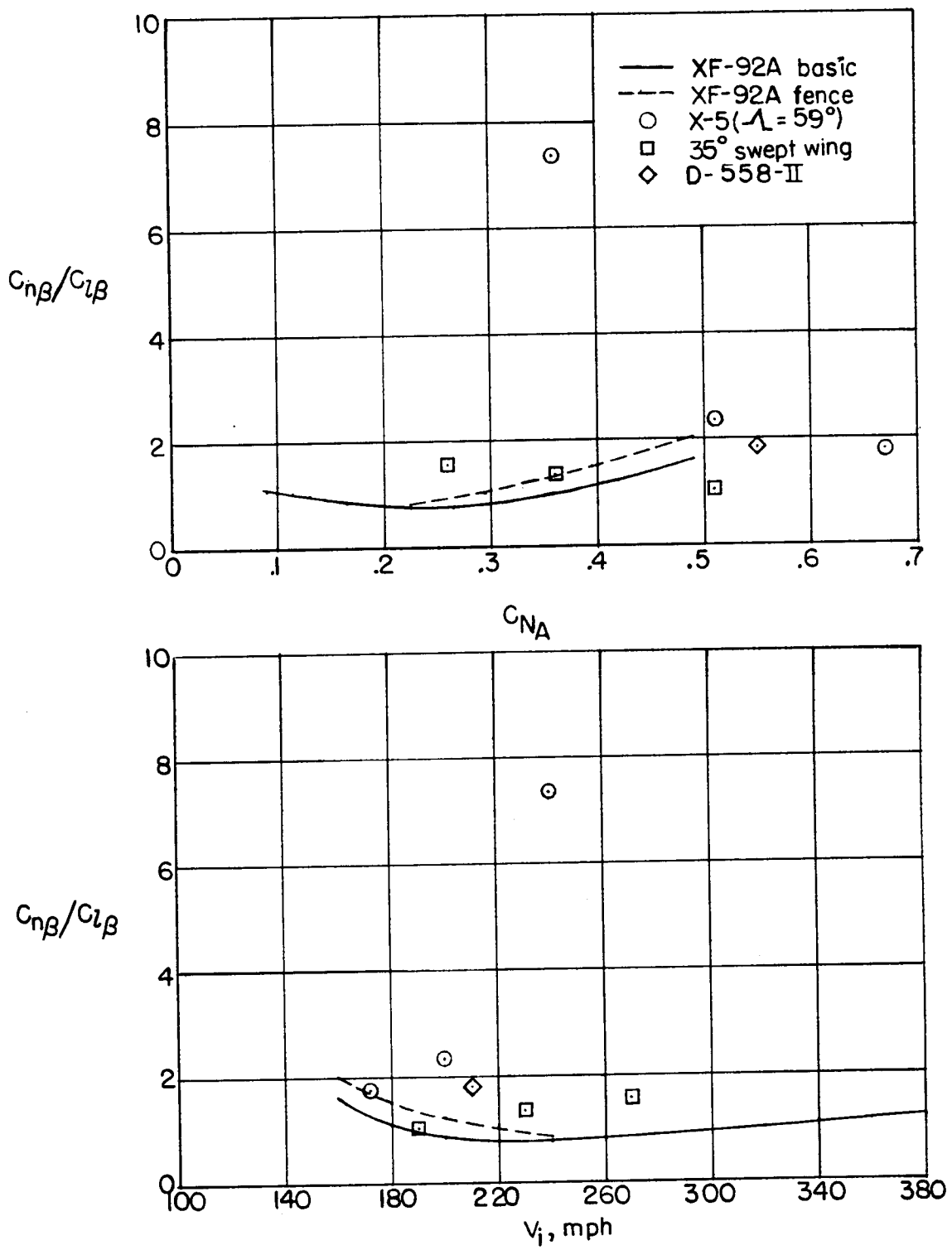

(a) C_{n_β}/C_{l_β} ratio.

Figure 18.- Variation of lateral stability derivative ratios with lift coefficient and indicated speed.

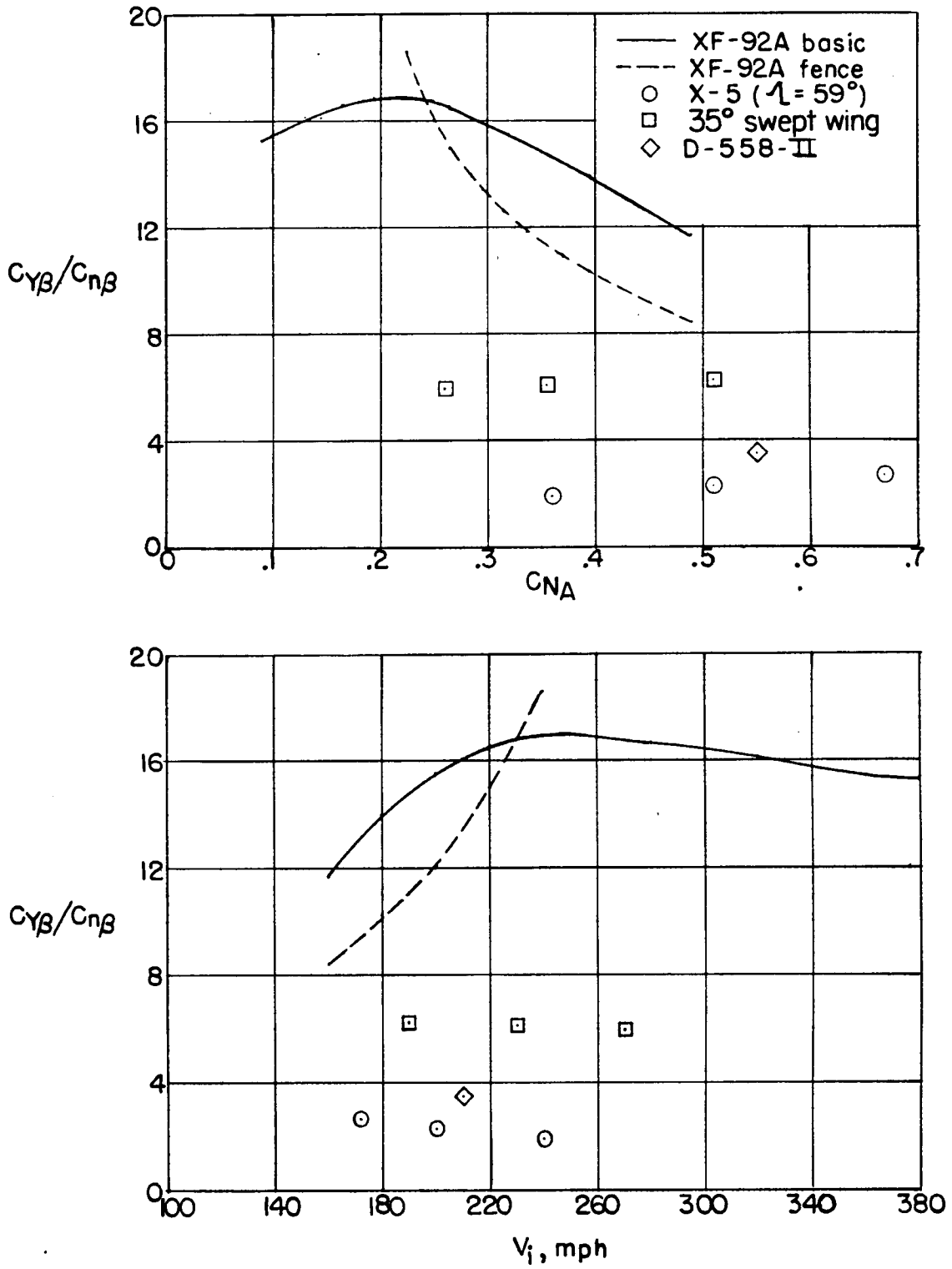

(b) C_{Y_β}/C_{n_β} ratio.

Figure 18.- Concluded.

NACA-Langley - 5-26-55 - 350